CHALMERS
UNIVERSITY OF TECHNOLOGY

Simulation for severity assessment of motor vehicle accidents

Master's Thesis in Mobility Engineering

ELIAS BÄCKLUND EKVALL & ERIK TINGFALK

Department of Mechanics and Maritime Sciences

CHALMERS UNIVERSITY OF TECHNOLOGY
Gothenburg, Sweden 2023
www.chalmers.se

Master's thesis 2023

Simulation for severity assessment of motor vehicle accidents

ELIAS BÄCKLUND EKVALL
ERIK TINGFALK

CHALMERS
UNIVERSITY OF TECHNOLOGY

Department of Mechanics and Maritime Sciences
Division of Vehicle Engineering and Autonomous Systems
Chalmers University of Technology
Gothenburg, Sweden 2023

Simulation for severity assessment of motor vehicle accidents
ELIAS BÄCKLUND EKVALL & ERIK TINGFALK

Supervisor: Xunbo Yang, Volvo Cars - Platform Design LVC (Longitudinal Vehicle Control)
Examiner: Mats Jonasson, Division of Vehicle Engineering and Autonomous Systems

Master's Thesis 2023
Department of Mechanics and Maritime Sciences
Division of Vehicle Engineering and Autonomous Systems
Chalmers University of Technology
SE-412 96 Gothenburg
Telephone +46 31 772 1000

Cover: Car following scenario visualized in IPG CarMaker.

Typeset in LaTeX
Printed by Chalmers Reproservice
Gothenburg, Sweden 2023

Simulation for severity assessment of motor vehicle accidents.
ELIAS BÄCKLUND EKVALL & ERIK TINGFALK
Department of Mechanics and Maritime Sciences
Chalmers University of Technology

Abstract

Battery electric vehicles (BEVs) exhibit distinct vehicle characteristics, including dynamics, increased mass, and acceleration capabilities. To assess the impact of BEVs on traffic hazard classification, a simulation model that accurately captures vehicle behavior in critical traffic scenarios is required.

This thesis presents the development and integration of a vehicle model within a traffic scenario simulation using Matlab/Simulink. The vehicle dynamic behavior of the model has been validated using IPG CarMaker, ensuring accurate representation.

The outcome of this research is a simulation model that covers both vehicle and driver behaviour in safety-critical situations. The model facilitates the determination of severity levels in the event of a system fault leading to unintended acceleration or deceleration of the vehicle.

The findings demonstrate that BEVs give rise to more severe situations, resulting in higher ASIL levels compared to internal combustion engine (ICE) vehicles. Consequently, the introduction of electric propulsion systems will alter the severity classification in common longitudinal scenarios.

In conclusion, this thesis emphasizes the transformative impact of electric propulsion systems on traffic hazard classification and establishes the significance of developing simulation tools that accurately capture the behavior of BEVs in safety-critical scenarios.

Keywords: Battery electric vehicles, Functional Safety, ISO 26262, Simulink, IPG CarMaker, vehicle dynamics.

Acknowledgements

First of all, we would like to thank Xunbo Yang and Nina Fredriksson at Volvo Cars, for their support during this thesis. They have supported us with their knowledge of functional safety and function development and we have been able to discuss ideas with them and been given valuable advice on what is important to focus on when it comes to developing models like this. We would also like to thank Mats Jonasson at Chalmers for being our examiner and with his vast experience of the automotive industry as a whole helping us set a good scope for the thesis and focus it on what's relevant for the future. He has also given us valuable insight into vehicle dynamics and helped us with vehicle modelling.

Elias Bäcklund Ekvall & Erik Tingfalk, Gothenburg, July, 2023

List of Acronyms

Below is the list of acronyms that have been used throughout this thesis listed in alphabetical order:

ADAS	Advanced Driver-assistance System
AEB	Autonomous Emergency Braking-system
ASIL	Automotive Safety Integrity Levels
ASM	Asynchronous Motor
BEV	Battery Electric Vehicle
CAN	Controller Area Network
E/E	Electrical and/or electronic
FDTI	Fault Detection Time Interval
FHTI	Fault Handling Time Interval
FMU	Functional Mock-Up Unit
FRTI	Fault Reaction Time Interval
FTTI	Fault Tolerant Time Interval
HMI	Human Machine Interface
ICE	Internal Combustion Engine
NHTSA	National Highway Traffic Safety Administration
PMSM	Permanent Magnet Synchronous Motor
QM	Quality Management
RMS	Root Mean Square
SHRP2	Strategic Highway Research Program 2
SOC	State of Charge
THW	Time Headway
VRU	Vulnerable Road Users

Contents

List of Figures

List of Tables

1

Introduction

This chapter will give an introduction to the thesis by first covering the background and objective together with an analysis of what has previously been done within the field of functional safety. Further, the research scope will be defined by covering the research questions and limitations of the project.

1.1 Background

Safety is a vital part of today's vehicle development, and it is concerning both the pre-crash phases and in-crash phases. In the pre-crash phase, sensors, actuators, and HMI (Human-Machine Interface) are used to form active safety systems and fully autonomous systems. The systems aim to mitigate and avoid crashes for road vehicles by in some way controlling or monitoring the longitudinal and lateral motion of the vehicle. During the in-crash phase the vehicle rely on it crashworthiness to mitigate the damages of the crash, this by how the vehicle is design with for example crumple zones.

Safety should always have a high priority when it comes to the development of cars. One method that can be used in vehicle development is to analyse different traffic scenarios and identify scenarios where a crash can happen and estimate the severity of the potential crash. With this knowledge, automakers can design safety mechanisms and systems aimed to avoid hazardous scenarios.

Volvo Cars produce among the safest cars in the world and the company is a leader in the field of car safety. They have been leading the safety field for decades and contributed to the development of new safety features for road vehicles. Longitudinal control is one of the attributes contributing to these safety systems. Longitudinal Vehicle Control involves the functions of acceleration and deceleration with a focus on creating safe, energy-efficient and rewarding longitudinal vehicle behaviour. The longitudinal control software has a high level of safety criticality where functional safety classification standards can be used. ISO 26262 (ISO Central Secretary, 2018) describes the requirements for functional safety in automotive applications. To know how to design the safest software it is required for Volvo Cars to understand how severe the potential traffic hazards can be. In order to do this a correct identification and classification of the hazardous event is crucial. This thesis investigates the possi-

bilities to build a model that can support the evaluation of hazard and classification levels, to design longitudinal control software in an early concept phase.

With the introduction of battery electric vehicles (BEV), several parameters and behaviours of the vehicle have been changed compared to an internal combustion engine (ICE) propelled car. This includes parameters of weight distributions, vehicle weight and most importantly acceleration capabilities. The increased acceleration capabilities could potentially have a huge impact on the classification of a traffic hazard, hence the need to develop a model for severity-level classification.

1.2 Objective

This master thesis includes identifying and investigating the most common longitudinal traffic hazard scenarios and then building a simulation model in Matlab/Simulink. The aim is to more accurately estimate the outcome of the hazard scenarios and the work is mainly focused towards an electric powertrain but a model for an ICE powertrain will also be used to evaluate differences. A necessary literature study is required in order to understand and set up the scope of the hazard scenario as well as the safety analysis process from ISO 26262. Testing and verification of the model will be performed by designing test events accordingly and trying to get a controllability level. Initial verification of the model will be performed by doing virtual simulations using IPG CarMaker. The second step of the verification process will be to perform a physical test using a test car.

1.3 Research Questions

The thesis will try to answer the following research questions:

- How will the severity assessment and FTTI for longitudinal scenarios change with the introduction of electric vehicles?
- What level of complexity is needed for a vehicle model to be used in risk assessment?

1.4 Previous Research

Research has been made by the National Highway Traffic Safety Administration (NHTSA) regarding functional safety of electric Vehicles. The research paper Functional Safety Assessment of a Generic Accelerator Control System With Electronic Throttle Control in Electric Vehicles (Becker et al., 2020) is an example of such research. In the report, NHTSA tries to find safety requirements related to the failures and countermeasures of the accelerator control system with electronic faults. The research suggests multiple Vehicle-level hazards connected to the accelerator control system. Table 1.1 show the seven identified hazards and their corresponding most severe ASIL (Automotive Safety Integrity Level) based on ISO 26262. This is one

example how a result from an ASIL analysis might look. Different OEM (Original Equipment Manufacturer) across the industry have their own way of making a complete ASIL analysis and shown below are Beckers result and not a industry wide consensus.

Table 1.1: Vehicle-Level Hazards and Corresponding ASIL, from Beckers report

	Hazard	ASIL
H1	Potential uncontrolled vehicle propulsion	D
H1.a	Potential uncontrolled vehicle propulsion when the vehicle speed is zero	B[i]
H2	Potential insufficient vehicle propulsion	C[ii]
H3	Potential vehicle movement in an unintended direction	C
H4	Potential propulsion power reduction/loss or vehicle stalling	D
H5	Potential insufficient vehicle deceleration	C[ii]
H6	Potentially allowing driver's command to override active safety systems[iv]	D[iii]
H7	Potential electric shock	B

Potential uncontrolled vehicle propulsion and potential propulsion power reduction/loss or vehicle stalling are identified as the most crucial hazards and thereby classified as ASIL D. Classifying the hazards is done by assessing the exposure, severity and controllability. Becker has made the classifications for controllability and exposure for each of the hazards based on ISO2626. For the first hazard in table 1.1 Becker has classified the exposure at E4 and controllability at C3, giving the ASIL level of D. NHTSA has managed to assign the different hazards with ASIL levels but addresses issues connected to this process. The report addresses a problem where the classification could differ between analysts due to the lack of objective data supporting the definitions of severity, exposure, and controllability. For the purpose of this thesis, those issues will not be a problem since the definitions of severity, exposure, and controllability already have been defined in internal standards at Volvo Cars.

Research investigating the severity difference between BEV and ICE vehicles is rare due to that BEV is new to the market and only recently gaining fleet penetration, in combination with the time required to retrieve crash data.

However, a few studies have been conducted comparing crash data between ICE vehicles and BEVs. One such study, based on crash data gathered in Norway, reveals that there is no notable difference in crash severity between BEVs and ICE vehicles. However, the study did highlight a significant increase in crash severity specifically for accidents involving motorcyclists and BEVs (Liu et al., 2022). There is also another report from Norway that implies that the weight of BEV might be a problem since it increases the injury severity of the vehicle you are colliding with (Høye, 2017).

Similar studies have been carried out to try and identify how you can classify the right severity, exposure, and controllability for hazards in longitudinal scenarios. One example is (Fabris & Lovric, 2012) where they showed how to get an ASIL level for unintended deceleration, to get severity accidents report was used, for exposure

data on where rear-end accidents took place was used and to get controllability driver behaviour was examined through analysis of brake distribution behaviour for different drivers.

1.5 Limitations

This thesis will only cover longitudinal control situations and potential traffic scenarios which exclusively involve behaviours in the longitudinal direction of the vehicle. An example could be a car following scenario on a straight road since this case does not include any lateral movements.

The possibility of verifying the simulation model in a physical test car setup will be limited since the situations to be simulated will cover the extremes of critical situations i.e. crashes. Test track verifications will be performed but cannot fully validate the model performance due to the complexity and safety risk of performing the tests.

2

Theory

This chapter will cover the relevant theory for the thesis which will include the concepts of functional safety and ISO 26262, traffic scenario modelling, vehicle modelling and driver modelling.

2.1 Functional Safety

Functional safety is the part of the overall safety of a product that depends on the correct functioning of a system. These safety functions are intended to prevent, or mitigate the consequences of, failures in the system that could lead to a dangerous situation. Besides functional safety, the overall product safety could also include mechanical and electrical safety. Electrical safety is different from functional safety in the way that functional safety is focused on ensuring that a system performs its intended safety functions, while electrical safety is focused on preventing hazards arising from the use of electricity. Both are important in ensuring the overall safety of a system or equipment (SÜD, n.d.).

Functional safety can be applied in a wide range of products ranging from buildings to industrial applications. The overall functional safety framework is described in the standard IEC 61508 (International Electrotechnical Commission, 2010) which covers all industries. The standard provides a systematic and structured approach for identifying and controlling hazards, and for ensuring that safety-related systems perform their intended safety functions under all conditions. Based on the standard IEC 61508 (International Electrotechnical Commission, 2010) each industry has its own adaptation summarized in a separate standard. For the automotive industry, the functional safety regulations are based on the standard IS0 26262 (ISO Central Secretary, 2018).

In an automotive application, functional safety is concerned with potential hazardous situation that might occur due to system malfunctions. Example of a malfunction can be that the vehicle loses its ability to break when the break pedal is pressed down, which can lead to a collision if there is a vehicle in front. Vehicle safety on the other hand is a broader term that includes all aspects of a vehicle's design and operation that contribute to the safety of the occupants and other road users. This includes not only safety-critical systems preventing accidents occurring in the

first place but also passive safety systems like crumple zones aiming to mitigate the consequences in the case of a crash.

2.1.1 ISO 26262

Automotive functional safety is based on the standard ISO 26262 (ISO Central Secretary, 2018) Road vehicles — Functional safety. This standard shall be applied to electrical and/or electronic (E/E) systems in production passenger cars and light commercial vehicles. The standard takes into account the specific safety requirements and the safety-related aspects of the automotive systems, as well as the safety-related aspects of the software. It addresses potential hazards in the case of a malfunctioning system. In an automotive setting, this could for example be a malfunctioning propulsion actuator resulting in torque demand too much or too less compared to the request from the driver.

2.1.2 ASIL classification

ISO 26262 uses a metric called Automotive Safety Integrity Level (ASIL) for classification of potential hazards. The respective level is connected to recommendations and actions needed to avoid and mitigate the consequences of a fault. The standard describes four different levels of risk, ranging from ASIL-A to ASIL-D, where ASIL-A describes a need for low-risk reduction and ASIl-D describes a need for high-risk reduction. An additional level called Quality Management (QM) is also available in cases where the risk has been reduced as a result of activities according to state of the art industry processes. In these cases, the risk can be managed and does not emphasize safety requirements to be managed under ISO 26262, instead one should use an industry-approved quality system (Aptiv, n.d.).

ASIL levels are determined by three factors: Severity, Exposure and Controllability. Severity describes the type of injuries to the driver and passengers and possible vulnerable road users (VRU). Table 2.1 shows the four levels of severity, S0 to S3 and their respective description (ISO Central Secretary, 2018).

Table 2.1: Severity classification

	Class			
	S0	**S1**	**S2**	**S3**
Description	No injuries	Light and moderate injuries	Severe and life-threatening injuries (survival probable)	Life-threatening injuries (survival uncertain), fatal injuries

The second factor is Exposure and it defines how often the individual is exposed to a situation. Table 2.2 shows the five levels of exposure, E0 to E4 and their respective description.

Table 2.2: Exposure classification

	Class				
	E0	**E1**	**E2**	**E3**	**E4**
Description	Incredible	Very low probability	Low probability	Medium probability	High probability

Controllability is the last factor determining the ASIL level and it defines how much the driver can do to prevent the injury by involvement in the operational situation. Table 2.3 shows the four levels of controllability, C0 to C3 and their respective description.

Table 2.3: Controllability classification

	Class			
	C0	**C1**	**C2**	**C3**
Description	Controllable in general	Simply controllable	Normally controllable	Difficult to control or uncontrollable

These factors are then combined according to Table 2.4 in order to determine the required ASIL level.

Table 2.4: ASIL determination

Severity class	**Exposure class**	**Controllability class**		
		C1	**C2**	**C3**
S1	**E1**	QM	QM	QM
	E2	QM	QM	QM
	E3	QM	QM	A
	E4	QM	A	B
S2	**E1**	QM	QM	QM
	E2	QM	QM	A
	E3	QM	A	B
	E4	A	B	C
S3	**E1**	QM	QM	A[a]
	E2	QM	A	B
	E3	A	B	C
	E4	B	C	D

2.1.3 Safety Goal

In the standard ISO 26262 safety goals are defined as top-level safety requirements for a function or item. These safety goals are defined in a project concept phase and used to define functional safety requirements that are aiming to prevent an unreasonable risk for a hazardous event. Each safety goal is assigned an ASIL and relevant requirements intended to bring the vehicle to a safe state if a failure occurs.

Fault Tolerant Time Interval (FTTI) is a necessary attribute of safety goals. FTTI is a time measure from the occurrence of a fault to the occurrence of a possible

hazardous event in the case where no safety mechanisms are present. If a system failure is present longer than the FTTI, a hazardous event will most likely occur. Figure 2.1 show the time definition of FTTI according to ISO 26262 (ISO Central Secretary, 2018) in a situation.

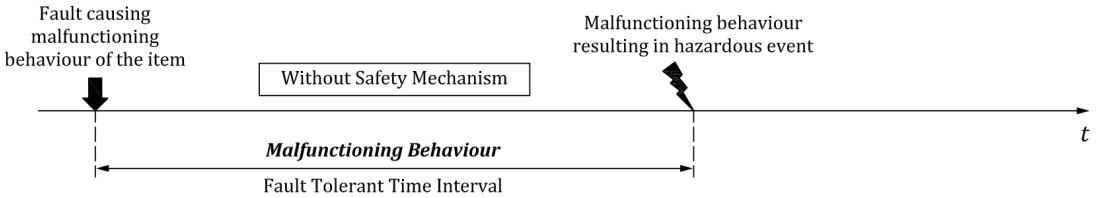

Figure 2.1: Illustration of FTTI definition according to ISO 26262.

In order to avoid a hazardous event from happening the Fault Handling Time Interval (FHTI) needs to be kept within the limit of FTTI. The FHTI is the sum of Fault Detection Time Interval (FDTI) and the Fault Reaction Time Interval (FRTI). Figure 2.2 show the definition of FHTI according to ISO 26262 (ISO Central Secretary, 2018).

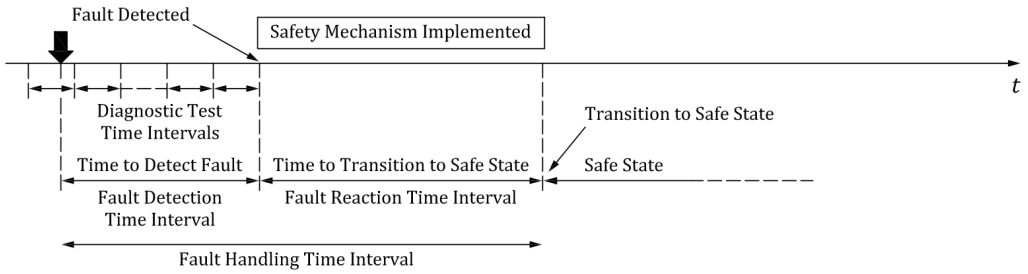

Figure 2.2: Illustration of FHTI definition according to ISO 26262.

In the case where a safe state cannot be reached within the FTTI, the system can enter emergency operation mode if such operation is defined. This mode is limited by the Emergency Operation Tolerant Time Interval (EOTTI) which is the time interval where a safe state needs to be achieved. Fig 2.3 shows the definition of FHTI in combination with an emergency operation according to ISO 26262 (ISO Central Secretary, 2018).

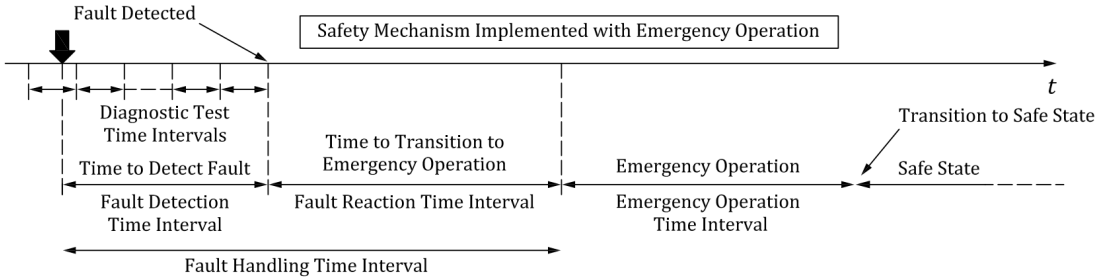

Figure 2.3: Illustration of FHTI definition according to ISO 26262.

2.2 Traffic Scenarios

This thesis will investigate both hazardous scenarios that can occur where two vehicles are following each other but also hazardous scenarios involving a Vulnerable Road User (VRU) and a car. The scenario chapter will first introduce general input parameters for the scenarios covering distance between cars at the start of the event, reaction time of the driver, road friction, and applied brake force. Furthermore, the scenarios will be described in detail covering the traffic scenario in combination with an assumed fault.

2.2.1 General input parameters

General parameters that will be used in this in investigating driver responses are reaction time and time headway (THW), reaction time will not be included to any large extent in this report but THW will be central.

Time headway seems to be unaffected by speed as shown by (Taieb-Maimon & Shinar, 2001) and (WINSUM & HEINO, 1996). This may give some input to what distances to assume by most drivers when it comes to car following scenarios, at least for speeds ranging from 50 km/h and upwards. Both these studies concluded that headway varies depending on the driver but for worst-case scenarios there might be time headway of below 1 second. (WINSUM & HEINO, 1996) found a comfortable time headway of 0.67 seconds and a standard deviation of 0.16 seconds for people that follow the lead car closely, while (Taieb-Maimon & Shinar, 2001) found an average comfortable time headway of 0.98s with a standard deviation of 0.36 s and the 5:th percentile at 0.45 seconds. The difference in these studies is that (WINSUM & HEINO, 1996) divided their result into groups depending on their perceived comfortable time headway. Notable also is that these are considered on rural roads under controlled environments and in simulators meaning they might not be relevant for close-range city driving.

A literature review carried out by (Green, 2000) which examined different publications on driver reaction times showed that unexpected events results in a response time of 1.5 seconds. This includes the time it takes to move from the gas pedal to the brake pedal which Green means can be estimated to 0.3 seconds for unexpected events. There are some differences among drivers and (Fambro et al., 1997) shows that a good estimation of the lower 5:th percentiles reaction time is around 2.5 seconds.

2.2.2 Scenario 1

This scenario is defined as a car-following scenario, involving two cars, a lead car and a following car. The lead car is driving at cruise speed on a straight road and the following car is following the lead car keeping a constant gap. Due to an undefined malfunction an unintended acceleration of the following car occurs and ends up in a potential rear-end striking of the lead car. Figure 2.4 illustrates the scenario.

Figure 2.4: Illustration of car following scenario with an unintended acceleration of the following car.

2.2.3 Scenario 2

This scenario is defined as a car-following scenario, involving two cars, a lead car and a following car. The lead car is driving at cruise speed on a straight road and the following car is following the lead car keeping a constant gap. Due to an undefined malfunction an unintended deceleration of the lead car occurs and ends up in a potential rear-end striking of the lead car. Figure 2.5 illustrates the scenario.

Figure 2.5: Illustration of car-following scenario with an unintended deceleration of the lead car

Within the automotive industry, two main definitions are used to describe the issues connected to brake system failures. The first one is defined as an overbraking situation meaning that the car brake system achieves more brake torque than what is requested. If a fault like this occurs there is a high risk of a rear impact by a following car. Underbraking is another system failure definition which means that the brake torque output is less than what is requested either from the driver or an Active safety system in the car. In a car following scenario the underbraking fault has a high potential of resulting in a rear-end crash into the car in front.

2.2.4 Scenario 3

This scenario involves one car and a VRU at a pedestrian crossing and the car is at standstill waiting for the VRU to cross. Due to an undefined malfunction an unintended acceleration of the car occurs and ends up in a potential collision with the VRU. Figure 2.6 illustrates the scenario.

Figure 2.6: Illustration of standstill scenario at a pedestrian crossing with an unintended acceleration of the car.

For this scenario to be used in a simulation the average distance between car and pedestrian needs to be defined. The Swedish Transport Administration defines regulations and recommendations for the design and construction of roads and streets. They recommend different values for the distance d illustrated in figure 2.7, between a pedestrian crossing and a stop line depending on the road situation. In the case of a signal-controlled intersection, the stop line should be placed at a minimum distance of 2 m from the pedestrian crossing but could in some cases be extended up to 5 m (Trafikverket, 2020).

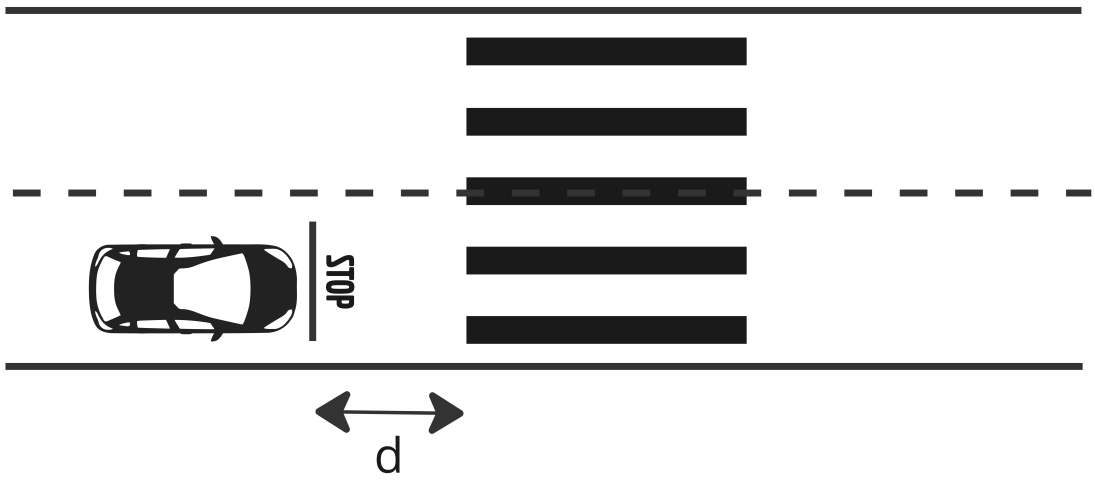

Figure 2.7: Illustration of pedestrian crossing design measure, d

2.2.5 Scenario 4

This scenario involves two cars at a roundabout or alternatively a crossing. Ego car is at standstill waiting for the other car to pass. Due to an undefined malfunction an unintended acceleration of the ego car occurs and ends up in a potential side impact collision. Figure 2.8 illustrates the scenario.

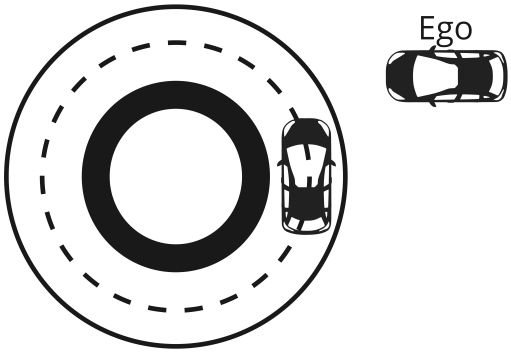

Figure 2.8: Illustration of standstill scenario at a roundabout with an unintended acceleration of ego car.

2.3 Vehicle Modeling

Following section will present relevant theories needed for the modelling of car behaviour. This includes:

Kinematic and dynamic models
Driving Resistance
Tire modelling
Propulsion forces
Electric powertrain
Suspension and load transfer

This thesis is only covering the longitudinal behaviour of the car and therefore all lateral properties of the car subsystems will be excluded. Figure 2.9 shows the car coordinate system definition only including the definitions needed for the longitudinal behaviour.

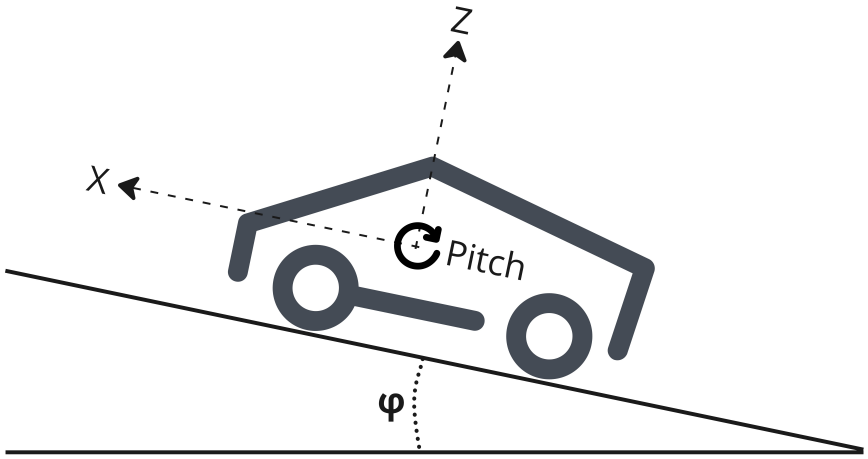

Figure 2.9: Car coordinate system definition

φ	Road inclination angle
θ	Chassi pitch

2.3.1 Kinematic and Dynamic models

Pointmass models are simple models that only consider the forces acting on the body. For a car, this could be air resistance and propulsion forces/braking forces on the tires. These models can be sufficient accurately to simulate some situations where the dynamic motion of the body does not contribute significantly or where some smaller errors are acceptable.

Dynamic models include the forces acting in the body, inertia for example. When only considering longitudinal forces in the case of car dynamics these forces will mainly affect the dive and pitch of a car during acceleration or deceleration.

2.3.2 Driving Resistance

Following equation can be used to calculate the resulting resistance acting on the car. The formula consists of gravitational force acting on the car due to road inclination, rolling resistance force from the tires and aerodynamic driving resistance force (Bengt J H Jacobson, 2020).

$$F_{resistance} = \underbrace{m \cdot g \cdot sin(\varphi)}_{F_{Gravitation}} + \underbrace{c_r \cdot m \cdot g \cdot cos(\varphi)}_{F_{RollResistance}} + \underbrace{\frac{1}{2} \cdot \rho \cdot A \cdot c_d \cdot v^2}_{F_{Aero}} \tag{2.1}$$

m	Vehcile mass
g	Gravitational constant
φ	Road inclination angle
c_r	Rolling resistance coefficient
ρ	Density
A	Area
c_d	Air resistance coefficient
v	Vehicle velocity

2.3.3 Tire modelling

Tire models are used to get an accurate behaviour of the tire during car simulations. Tires are hard to model and if to be precise can be very computationally expensive. There are however different empirical tire models that have relatively low complexity and give a good estimation of the tire behaviour. One of these models is the Pacejka "Magic tire formula" (Pacejka, 2012) which relies on empirical data together with

the tire's individual characteristics. The model assumes that a curve for slip-friction retains its shape when running in different conditions to the tested and can therefore be used in a variety of situations based on the same parameters. In this thesis, this model will be used to estimate the force that can be utilized to decelerate or accelerate the car. Thus, this thesis is mainly interesting in the acceleration and deceleration of a car the tire model used will be for pure longitudinal force.

Equation 2.2 is used to approximate the longitudinal force with constant coefficients. Variables B, C, D, and E are the parameters used to define the curvature of the slip-friction tire curve. These parameters are for the constant parameter formula given by table 2.7.

$$F_x = F_z \cdot D \cdot sin(C \cdot atan(B\kappa - E[B\kappa - atan(B\kappa)])) \tag{2.2}$$

Where κ is the longitudinal slip which is the ratio between the difference of the velocity at the tire edge and the car divided by the maximum velocity of the car or velocity at the tire edge.

$$\kappa = \frac{Rw - vx}{\max(|Rw|, |v_x|)} \tag{2.3}$$

Table 2.7: Constant Magic Formula coefficients depending on surface type (Pacejka, 2012).

Surface	**B**	**C**	**D**	**E**
Dry tarmac	10	1.9	1	0.97
Wet tarmac	12	2.3	0.82	1
Snow	5	2	0.3	1
Ice	4	2	0.1	1

The longitudinal force can also be calculated using the Magic formula with load-dependent coefficients according to equation 2.4. For this case, the coefficients are calculated using tyre parameters given from tyre testing. B represents the stiffens, C is the shape, D peak value of the curve and E the curvature/form. κ in this case is the slip, the ratio between the velocity of the car and the velocity of the tire's outer edge. S_{Vx} is the vertical shift, this is to allow the slip curve to pass through the origin at zero slip. This slip is used to calculate the available friction which can be used to generate force to propel the car forward. For a full set of equations on how to drive the parameters B, C, D and E see Appendix A.

$$F_{x0} = D_x sin[C_x atan B_x \kappa_x - E_x(B_x\kappa_x) - atan(B_x\kappa_x)] + S_{Vx} \tag{2.4}$$

Where κ_x can be calculated as:

$$\kappa_x = \kappa + S_{Hx} \tag{2.5}$$

F_x	Force x direction
F_z	Normal force
F_{x0}	Force x direction
B_x	Formula parameter
C_x	Formula parameter
D_x	Formula parameter
E_x	Formula parameter
κ	Longitudinal slip
R	Tire radius
w	Angular velocity wheel
v_x	Velocity car x direction
S_{Vx}	Vertical correction factor
S_{Hx}	Horizontal correction factor
B_{reff}	Vertical reference

Here κ is the same as in previous magic formula and S_{Hx} is a horizontal correction factor to compensate so the slip-friction curve passes through the origin when changing sign when going from acceleration to deceleration. This can be seen in figure 2.10.

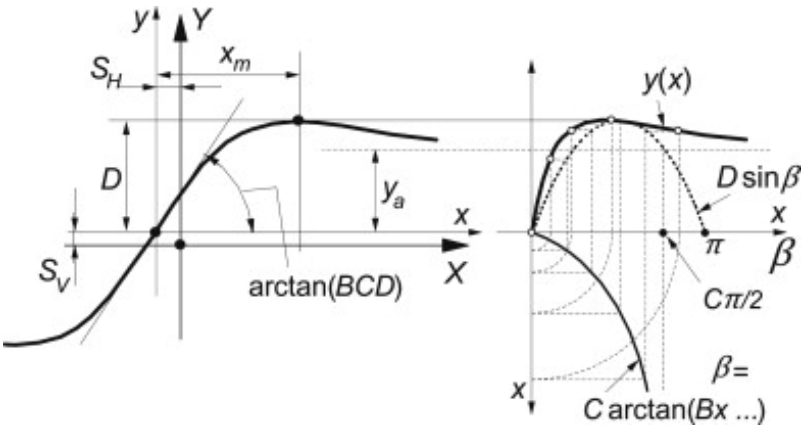

Figure 2.10: Slip friction curve, with representations of parameters. (Pacejka, 2012)

During driving the tire will deform and change its radius. The radius of the wheel can be approximated using the following equations. These use the normal load on the tire together with the vertical stiffens of the tire, reference values F, D, and B, where B is a reference for low load, F for high load and D, is the peak rolling radius.

$$r_e = r_\Omega - \frac{F_{zo}}{C_0}(F_{reff}\frac{F_z}{F_{z0}} + D_{reff} \cdot atan(B_{reff}\frac{F_z}{F_{z0}})) \tag{2.6}$$

R_e	Effective rolling radius
R_ρ	Free rolling radius
F_{z0}	Rated load
C_z	Vertical stiffness
F_z	Normal load
F_{reff}	Vertical reference
D_{reff}	Vertical reference
B_{reff}	Vertical reference

2.3.4 Propulsion forces

To propel the car forward power need to be transmitted from the engine to the wheel. Later in section 2.3.5 there will be explained how the power from the engine transfers to torque at the wheel, in this section the equations used to derive the force available to propel the car will be explained (Bengt J H Jacobson, 2020).

For a free body of a driven wheel, the acceleration of the wheel can be seen as:

$$J\dot{w} = T - FR \tag{2.7}$$

Thus F can be calculated as:

$$F = \frac{T - J\dot{w}}{R} \tag{2.8}$$

From the above equations, w can also be derived by taking the integration of:

$$w = \int \frac{T - FR}{j} \tag{2.9}$$

J	Wheel inertia
$\dot{w}$	Rotational acceleration of the wheel
F	Force at the wheel road contact point
R	Radius of the wheel

w will be used for calculating the slip for the tire modeling later on.

2.3.5 Electric powertrain

Battery Electric Vehicle (BEV) with an All-Wheel Drive (AWD) propulsion setup typically uses two electric motors, one on each axle. Where the rear axle motor most often is of the type PMSM (Permanent Magnet Synchronous Motors) and the front axle drive motor can be both type PMSM or ASM (Asynchronous motor). The torque speed characteristics for a typical PMSM can be seen in figure 2.11. The figure shows how the motor can supply instant torque from start and operate above rated torque. Torques above the rated operation of the electric motor can be delivered during shorter periods and therefore allow higher peak performance and acceleration capabilities (Hughes & Drury, 2019).

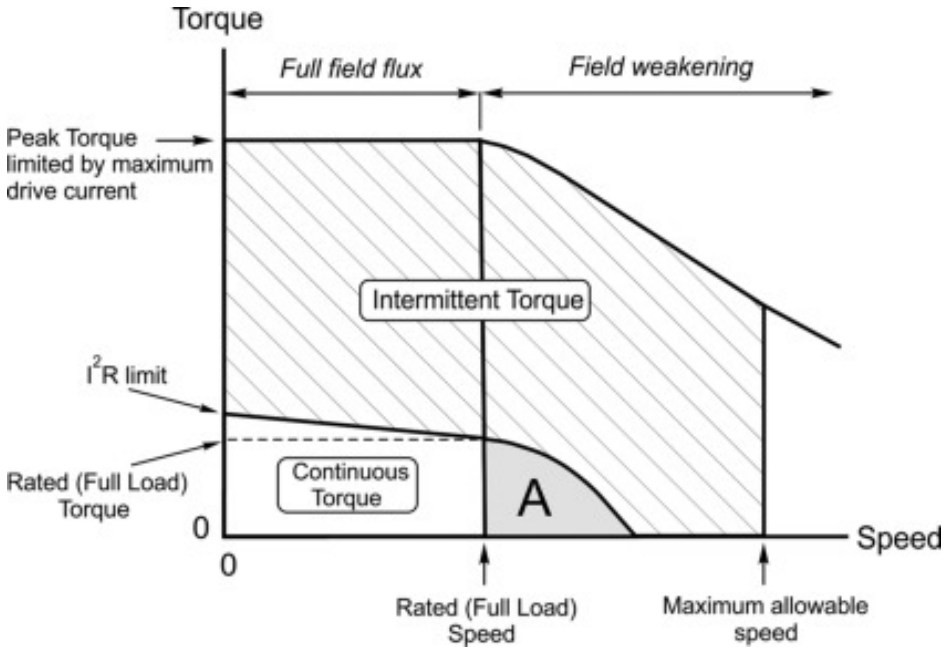

Figure 2.11: Plot illustrating the torque-speed characteristics of a typical PMSM (Hughes & Drury, 2019).

Powertrain modelling can be complex and require data on the parts making up the powertrain. Since this work is not interested in how the power transfers from the motor to the wheels nor where the losses occur, it's mostly interested in the time delay from when the power is requested until it refaces the wheels and the total loss. Test data with these values will be used instead of simulating or computing these losses.

For the modelling of the electric motors, we are only interested in the peak torque capabilities based on motor rotational velocity. This means that the electric motor can be modelled very simply by just mimicking the max torque behaviour based on a few input parameters. This simplifies the simulation by not modelling the complete propulsion system including batteries, inverters and electric motors.

Figure 2.12 shows a model approximation of a max torque request applicable both

for a Permanent Magnet Synchronous Motor (PMSM) and an asynchronous motor (ASM). The torque behaviour is assumed to be equal between the PMSM and the ASM for model simplification purposes. A build-up time is included to compensate for delays and limitations of electric current supply from the inverters and batteries. This time delay can be up to 400 ms.

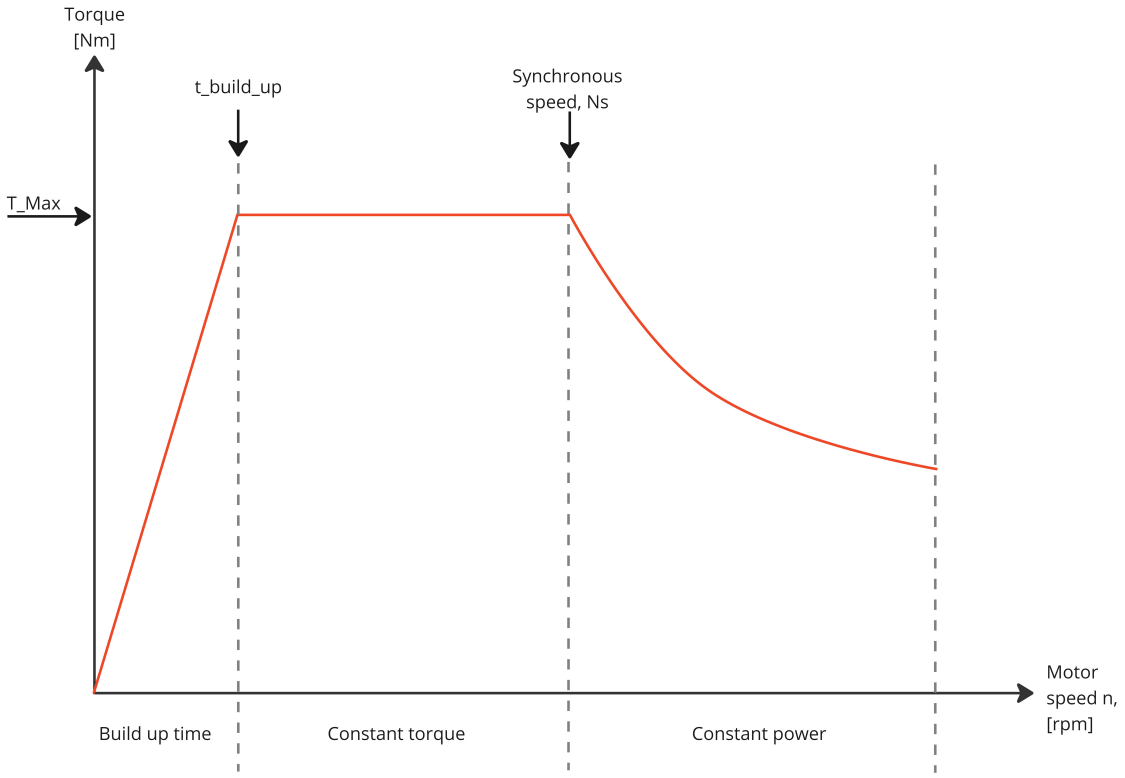

Figure 2.12: Plot illustrating the max torque characteristics of the EM.

Based on three parameters, rated max torque T_{max}, build-up time $t_{buildup}$ and Synchronous speed n_s, the torque behaviour can be approximated using equation 2.10.

$$T(n_r) = \begin{cases} = \frac{\Delta T}{\Delta n_r} \cdot n_r, \text{ during build up until } T_{max} \text{ is reached} \\ = T_{max}, \text{ for } n_r(t_{buildup}) < n_r < n_s \\ = \frac{P_{max}}{\Omega_r}, \text{ for } n_r > n_s \text{ where } P_{max} = T_{max} \cdot n_s \cdot \frac{\pi}{30} \end{cases} \tag{2.10}$$

n_r	Mechanical speed of the rotor [rpm]
n_s	Mechanical Synchronous speed [rpm]
$\Omega_r = n_r \cdot \frac{\pi}{30}$	Mechanical speed of the rotor [rad/s]
T_{max}	Rated max torque motor shaft [Nm]
P_{max}	Rated max power [w]

2.3.6 Suspension and load transfer

For realistic acceleration and deceleration curves, a full suspension model would be needed. Suspension models are however detailed and generally complex to involve, where more data about the car needs to be known to adjust for anti-dive and anti-squat mechanisms for example. These geometries will not always be available early in development. Therefore a part of this thesis is to evaluate if suspension modelling would be required to get a satisfactory result or not.

A simpler suspension model could be derived by taking the forces around the axle pivot points. This will include the suspension and load transfer of the car when accelerating and decelerating. With the load transfer correctly modelled there will be a more realistic result since the normal load on the wheels dictates how much force can be utilized to drive the car forward. The equilibrium equations around the front and rear pivot points which can be used to calculate the normal load given the force on the wheels from the ground are (Bengt J H Jacobson, 2020):

Equilibrium of forces longitudinal direction, horizontal with the road are.

$$-m\dot{v}_x + F_{xf} + F_{xr} = 0 \tag{2.11}$$

Equilibrium of forces vertical direction, assuming level road.

$$-m(\dot{v}_z + w_y v_x) - mg + F_{zf} + F_{zr} = 0 \tag{2.12}$$

Equilibrium of moment around the center of gravity.

$$-J\dot{w}_y + F_{zr}l_r - F_{zf}l_f - (F_{xf} + F_{xr})h = 0 \tag{2.13}$$

Equilibrium of moment around the pivot points, rear and front.

$$(F_{zr} - F_{sr} - F_{dr})g_r - F_{xr}e_r + T_{sr} = 0 \tag{2.14}$$

$$(F_{sf} + F_{df} - F_{zf})g_f - F_{xf}e_f + T_{sf} = 0 \tag{2.15}$$

Damper force equations front and rear.

$$F_{df} = -d_f v_{zf} \tag{2.16}$$

$$F_{dr} = -d_r v_{zr} \tag{2.17}$$

Spring force equation front and rear.

$$F_{sf} = F_{sf0} - c_f z_f \tag{2.18}$$

$$F_{sr} = F_{sr0} - c_r z_r \tag{2.19}$$

Visualisations of the forces can be seen in fig 2.13. Which shows the forces acting on the car and a representation of a wheel using a pivot point. Note that the e and g in the figure are representing the distance from the wheel centre to the pivot

point in x and y. T_s is the torque supplied directly to the shaft which typically is regenerative braking or torque from the engine.

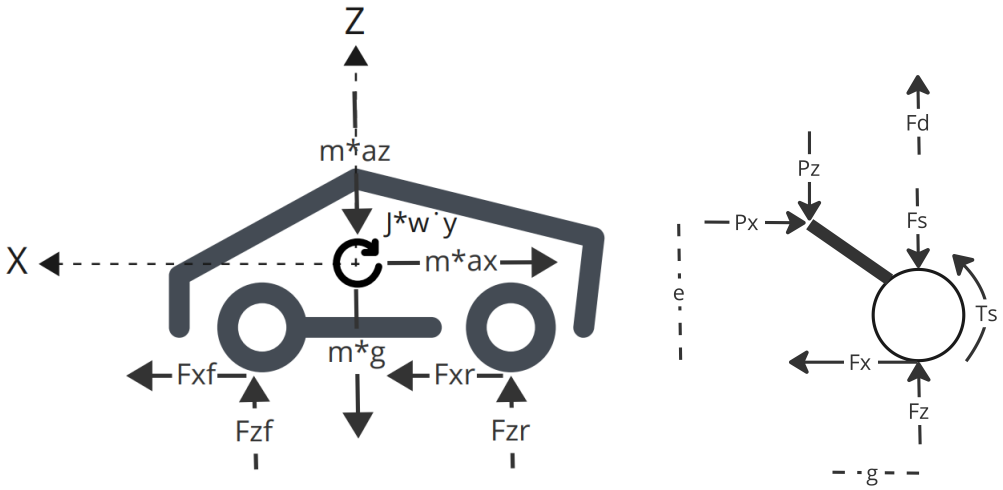

Figure 2.13: Acting forces on the car.

m	Mass
$\dot{v}_x$	Acceleration in x direction
F_{xf}	Force front in x direction
F_{xr}	Force rear in x direction
$\dot{v}_y$	Acceleration y direction
w_y	Rotational velocity around y axis
g	Gravity
F_{zf}	Normal force on front tires
F_{zr}	Normal force on rear tires
J	Inertia around y
$\dot{w}_y$	Rotational acceleration around y axis
l_r	Length from centre of rear wheel to centre of gravity
l_f	Length from centre of front wheel to centre of gravity
h	Height of centre of gravity
F_{sr}	Spring force rear
F_{dr}	Damper force rear
g_r	Length from pivot point to rear centre of rear wheel
e_r	Height from the ground to pivot point
T_{sr}	Shaft torque rear
F_{sf}	Spring force front

F_{df}	Damper force front
g_f	Length from pivot point to front centre of rear wheel
e_f	Height from the ground to pivot point front
T_{sf}	Shaft torque front
d_f	Damper coefficient front
v_{zf}	Velocity in z-direction front
d_r	Damper coefficient rear
v_{zr}	Velocity in z-direction rear
F_{sf0}	Initial spring force front
c_f	Spring coefficient front
z_f	Displacement spring front
F_{sr0}	Initial spring force rear
c_r	Spring coefficient rear
z_r	Displacement spring rear

2.4 Driver Modelling

Driver modelling is a crucial component in the development of virtual simulation environments enabling true human behaviour in multiple driving situations. The driver model can for example be used to predict and evaluate the behaviour of a human using an ADAS system. Multiple use cases and versions of driver models exist covering different kinds of behaviours covering reactions times, glance behaviour, pedal moment etc.

For this thesis, human behaviour concerning reaction times and braking behaviour during crucial situations is needed to be included in the simulation model. A model for the driver behaviour of the rear car in critical longitudinal scenarios with a slower or braking lead car is described in the research paper article "A quantitative driver model of pre-crash brake onset and control" (Svärd et al., 2017). The model is made to be used in simulations of critical longitudinal scenarios with a model output of brake initiation timing and brake jerk. Based on naturalistic near-crashes and crashes an accurate model has been developed covering the behavior of the driver in the scenario described. The research suggests that the kinematics of the lead car has the greatest impact on both brake initiation and brake ramp-up. This connection can be described with the concept of visual looming quantified in equation 2.20. Looming is the rate of change in size of the vehicle in front and can be seen as how fast a driver is perceiving the front vehicle to get closer or further away.

$$\tau^{-1} = \frac{\dot{\theta}}{\theta} \tag{2.20}$$

The variable θ refers to the width, or optical size, of the lead car as perceived by the driver's retina.

The model philosophy is that the driver gathers evidence for the first brake onset by continuously accumulating looming information and the driver is then assumed to apply the brake pedal once the accumulated evidence surpasses a predefined threshold. During the braking operation, the driver continually makes a prediction of how the looming will change due to the braking. The prediction is then compared to the actual looming perceived and a braking response is then issued based on the error.

Equation 2.21 describes the relation for the brake initiation, where $A(t)$ is defined as the total accumulated prediction error. If this value surpasses a predefined threshold a brake initiation will start. $\epsilon(t)$ is the total looming prediction error at time t, it is the error between the actual looming and the predicted looming adjustment calculated later see equations, 2.26. It can be said to be the result of current looming and predicted effect of the action taken by the driver. K and M are free model parameters. M represent the gating which can be seen as the minimum looming value to start accumulating evidence towards the need for a break response. This can be seen in equation 2.21 if $K \cdot \epsilon(t)$ is lower than M the model relies on eventual noise to take action. $v(t)$ is Gaussian zero-mean white noise meant to replicate the difference in behaviour between humans mainly concerning reaction times.

$$\frac{dA(t)}{dt} = K \cdot \epsilon(t) - M - C \cdot A(t) + v(t) \tag{2.21}$$

Equation 2.22, Equation 2.23, and Equation 2.24 describe the modulation part of the brake response, where g is the magnitude of each individual adjustment dependent on the looming prediction error and a free model parameter k. $G(t)$ is determining the shape of each brake adjustment and $C(t)$ gives the total brake pedal signal expressed in percentage from 0 to 100 based on the sum of all brake adjustments.

$$g_i = k \cdot \epsilon(t_i) \tag{2.22}$$

$$G(t) = \begin{cases} 0, \text{for } t \leq 0 \\ 1, \text{for } t \geq \Delta T \end{cases} \tag{2.23}$$

$$C(t) = \sum_{i=1}^{N} g_i G(t - t_i) \tag{2.24}$$

Equation 2.25 and Equation 2.26 describe the looming prediction that is fed back into the accumulator, where P_{P1} is the sum of the predicted resulting looming based on the previous brake adjustments.

$$H(t) = \begin{cases} = 0, \text{for } t \leq 0 \text{ and } t \geq \Delta T_p \\ \rightarrow 1, \text{for } t \rightarrow 0^+ \\ \rightarrow 0, \text{for } t \rightarrow \Delta T_p \end{cases} \tag{2.25}$$

$$P_{P1}(t) = \sum_{i=1}^{N} \epsilon(t_i) H(t - t_i) \tag{2.26}$$

2.4.1 Monte Carlo simulation

Monte Carlo simulation is a statistical method used to approximate a solution by using randomly generated numbers to solve a problem. The method gives a probability of different outcomes based on the randomly generated input parameters (Johansen, 2010). To get an accurate result distribution a large number of simulations needs to be performed. Depending on the amount of free variable parameters the needed simulation iterations will change but it is stated that at least 1000 iterations should be used. This is a trade off situation where accuracy needs to be balanced against computational resources.

The driver model described can be used in a Monte Carlo simulation to generate a distribution over brake response in different scenarios. The distributions would describe the different responses between humans due to multiple factors like age, fatigue, and distractions among other factors.

2.4.2 Deceleration distribution

Drivers tend to have different minimum decelerations in critical rear-end scenarios therefore using one single value will be a simplification of the situation. For a more accurate result, a distribution of seen maximum deceleration was used, the deceleration distribution comes from (Bärgman et al., 2017) and is from the SHRP2 dataset.

3

Methods

This chapter will cover the methods and tools used in this thesis including simulation setup for both MATLAB/Simulink and IPG CarMaker. The purpose and overall design setup of the simulation model will be described and how it can be verified with the use of IPG CarMaker.

3.1 Simulation and Modeling setup

For the simulation and modelling of crash scenarios, two main tools were used. MATLAB (The MathWorks Inc, 2021) in combination with Simulink was used in the development of a point mass model and IPG CarMaker (IPG Automotive GmbH, 2021) was used for reference and validation of the Simulink model. The following section will explain the tools and how they were used in this thesis.

3.1.1 MATLAB/Simulink

MATLAB is a powerful computation software used by scientists and engineers for analyzing data, developing algorithms, and creating models. Simulink is an extension to the MATLAB interface enabling simulations and model-based design by a graphical block diagram environment. Algorithms and variables from MATLAB can be used in the Simulink environment for the purpose of system simulation. Simulation results can then be stored in the MATLAB environment for further post-processing of data.

For the development of an easy-to-use simulation model, MATLAB/Simulink was used for the development of a point mass model since the software is easily accessed and widely used within Volvo Cars. Setting up each traffic scenario by representing vehicles as point masses simplifies the simulation and results in a model that can give a fast response to the user. The difficulty is to develop a model that is simple enough but still accurate compared to real-world situations.

The simulation model in Matlab/Simulink was set up with the goal of delivering an ASIL classification based on a set of input parameters. In order to archive this, three main components needed to be included in the simulation model. An accurate model of the vehicle behaviour covering vehicle dynamics, powertrain behaviour and

tire behaviour. The vehicle model was then included in a scenario model covering the ego vehicle together with the target vehicle and their interactions with each other depending on the scenario type. On top of these two components, a driver model was also included for the purpose of achieving a high-fidelity behaviour of a human handling a critical traffic situation. Figure 3.1 shows the simulation model setup and workflows.

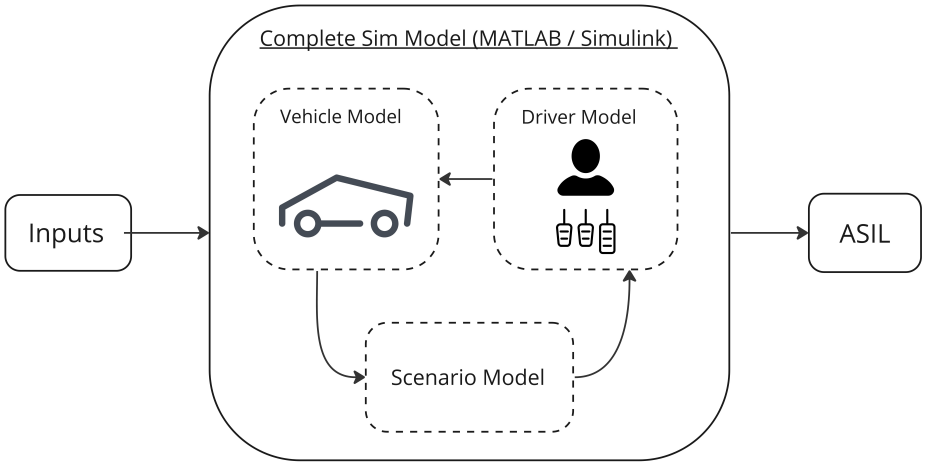

Figure 3.1: Simulation model setup

3.1.2 IPG CarMaker

IPG CarMaker is a software tool enabling virtual simulations of vehicle dynamic behaviour for complete car setups. The software includes advanced car models, driver models and multiple environment setup possibilities for roads and traffic. This enables the user to set up realistic test scenarios simulating vehicle manoeuvres and behaviour. CarMaker also includes the possibility of triggering different malfunctions at a given time.

IPG CarMaker models representing existing car models and cars currently in development were provided by Volvo Cars. The models use high-fidelity plugins and FMU:s of vehicle systems like suspension models, powertrain models and brake models. These systems can also be coupled to real software running on virtual ECUs creating a virtual simulation environment with very high fidelity.

The tool was mainly used for reference and validation of the Simulink model by setting up defined traffic scenarios and evaluating its performance. Two main scenarios were used in the verification of the vehicle behaviour of the Simulink model. The first scenario defined in CarMaker represents an unintended acceleration from various start speeds by triggering a digital max torque request on the ERAD and EFAD simultaneously. The second scenario represents an unintended deceleration from various start speeds by digitally triggering a max friction brake torque request. Relevant simulation parameters were then exported to Matlab for comparison with the Simulink model performance.

4

Results

In this chapter, the main results will be presented by first covering a verification of the vehicle model followed by a presentation of the complete simulation model and its severity estimation results for the four traffic scenarios. Furthermore, a severity assessment comparison between an ICE vehicle and a BEV will be presented.

4.1 Vehicle model verification

The following chapter will present the results from the verification of the vehicle model covering both the acceleration and deceleration behaviour of the model in comparison with the reference from IPG CarMaker. During verification, both models with and without suspensions is shown to see how they both compare towards each other and compared to IPG CarMaker, the model used for the complete simulation and thus also for estimation of severity and FTTI calculation is without suspension.

4.1.1 Deceleration

The vehicle model verification for the case of an unintended deceleration was made simulating a maximum brake torque request from a certain set speed assuming equal model performance for all start speeds. A comparison between the developed Simulink model for a BEV, both including and excluding suspension dynamics and the reference model from CarMaker can be seen in figure 4.1. The figure shows that the model generally covers the braking behaviour well over the whole braking sequence, with a RMS value of 0.3127 and 0.3396 for the model with suspension and the model without suspension respectively.

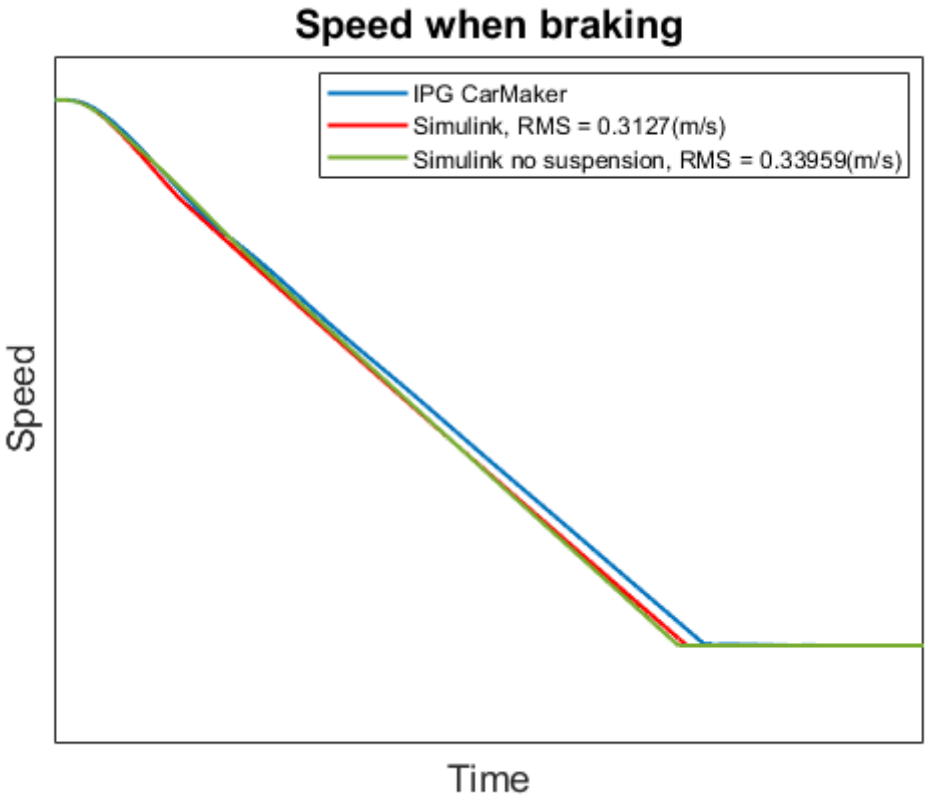

Figure 4.1: Deceleration performance showing the reference model and the developed Simulink model for a BEV.

Figure 4.2 shows the importance of suspension modelling for accurate wheel slip behaviour during the beginning of the braking manoeuvre. For the front axle wheel slip the result is improved with the addition of suspension modelling but does not fully replicate the reference. Rear wheel slip behaviour shows an even greater impact with the addition of suspension to the Simulink model.

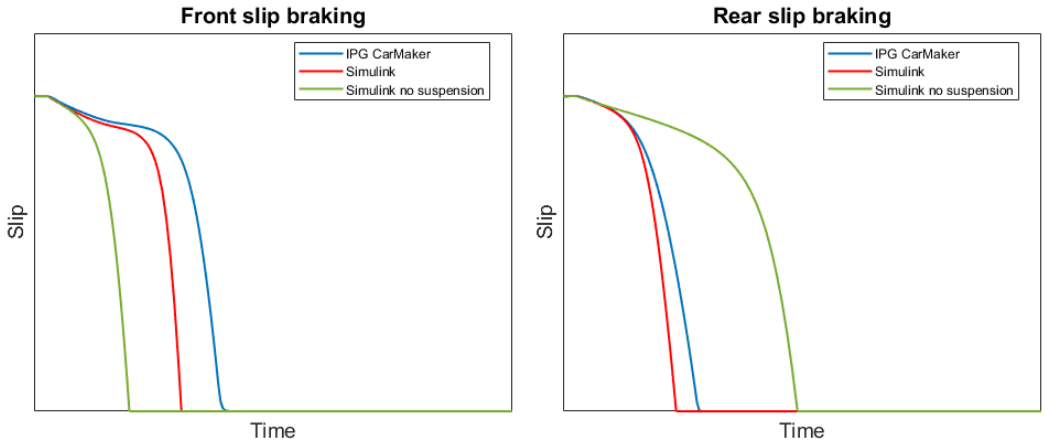

Figure 4.2: Front and rear wheel slip behaviour during deceleration for a BEV.

For the braking case, it can be concluded that the inclusion of suspension is crucial to receive an accurate slip behaviour of the wheels. For the purpose of this thesis and the intended use of the model, it was concluded that the inclusion of suspension is not necessary since the speed behaviour over the complete braking sequence is still matching the reference well enough. This decision simplifies the model making it less computationally costly and also reducing the number of input parameters needed to run the simulation model.

4.1.2 Acceleration

The vehicle model was also verified for an unintended acceleration scenario by simulating a digital maximum torque request from a certain cruise speed assuming the same model performance for all start speeds. A comparison between the developed Simulink model, both including and excluding suspension dynamics and the reference model from CarMaker can be seen in figure 4.3. The figure shows that the Simulink model replicates the reference behaviour accurately with an RMS value of 0.2939 and 0.2942 for the model with suspension and the model without suspension respectively. This resulted in the decision that the Vehicle behaviour can accurately be modelled without suspension and can therefore be excluded from the model.

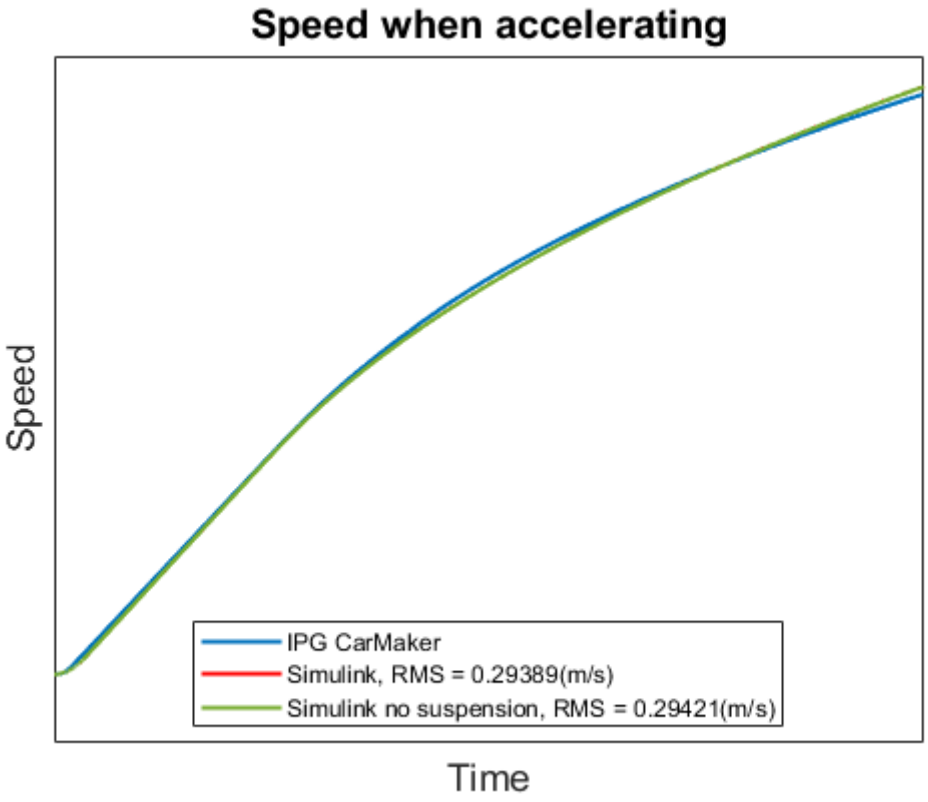

Figure 4.3: Acceleration performance showing the reference model and the developed Simulink model.

4.2 Complete model simulation

Figure 4.4 shows the Simulink model for an unintended acceleration scenario. This is an overview figure of the whole Simulink model which highlights the three main subsystems, being the car model, scenario model and driver model subsystem. The vehicle model produces the force used to propel the car and when resistance forces are subtracted acceleration can be derived. It calculates propulsion force using a torque curve from the engine combined with a wheel + tire model. Resistance forces can be calculated as mentioned in the theory. The ego speed and initial/lead car speed are then forwarded to the scenario which holds the relative speed between the cars and the distance between them. From that tau inverse can be calculated which is forwarded to the driver model which uses tau inverse to get a pedal response which is converted to a declaration level fed into the vehicle model. For all simulations, THW will be used to set the initial distance between the cars and is set to 1.5 sec which is longer than research shows but shorter than recommended.

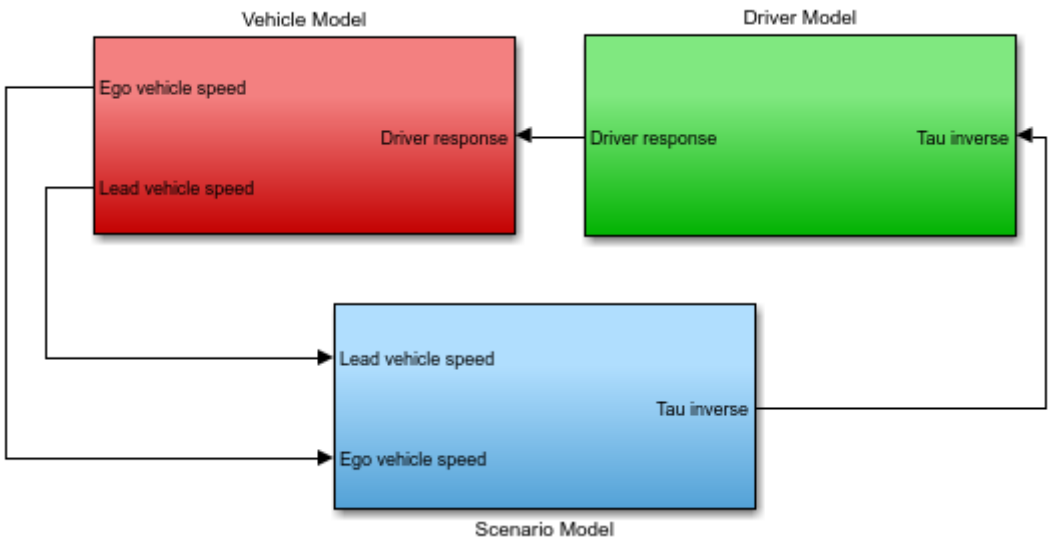

Figure 4.4: Overview of complete Simulink model

The models for the other scenarios follow the same three main subsystems, but each subsystem themselves differs depending on what simulation is running. For example, if the simulation is regarding a braking case the vehicle model differs to simulate the behaviour and delays of the braking system instead of the propulsion systems.

4.2.1 Unintended acceleration

Following section will present the result for the two cases regarding unintended acceleration. As described earlier the cases are unintended acceleration while in a car following scenario and from a standstill to a pedestrian crossing.

4.2.1.1 Car following scenario

Figure 4.5 shows the result for vehicle following vehicle scenario, whit the initial conditions of initial speed x-axis and maximum allowed acceleration y-axis. The plot shows the resulting severity classification based on the value from the x and y-axis. The simulation yields no severity for any case and all result in a no crash. Therefore there cannot be any FTTI for any speed, or maximum acceleration combination as there are no crashes. The values are taken after running a monte carlo simulation of 500 simulations for each speed-maximum acceleration combination and then the middle delta v value is selected. Meaning there could be some crashes recorded as will be seen in table 4.1 but since there are not more than fifty percent crashes the result will be a no crash.

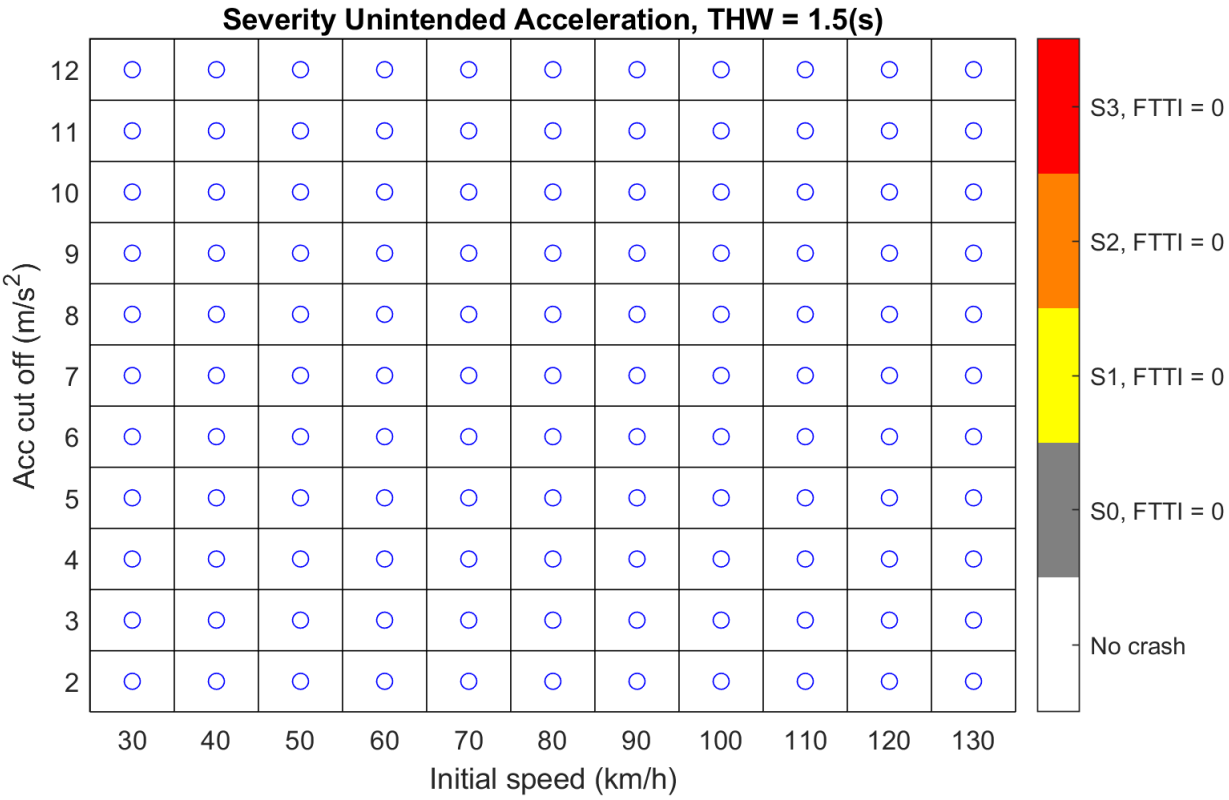

Figure 4.5: Severity classification plot for unintended acceleration in a car to car following scenario

Table 4.1 shows a part of the data used to create figure 4.5 Here are the percentages of crashes that occurred within each severity and the FTTI corresponding to the 250:th simulation (500 total simulations, 500/2 = 250). This value is chosen to get the most probabilistic severity from the scenario for a set initial speed and allowed acceleration. This means that there can occur some crashes but as seen in fig 4.5 the outcome will still yield a no-crash result.

Table 4.1: Severity and FTTI for the 10 first combinations of max acceleration and start speed.

Case	S0	S1	S2	S3	FTTI
"Max aceleration = 2, Speed = 30"	0	0	0	0	0
"Max aceleration = 2, Speed = 40"	0	0	0	0	0
"Max aceleration = 2, Speed = 50"	0	0	0	0	0
"Max aceleration = 2, Speed = 60"	0	0	0	0	0
"Max aceleration = 2, Speed = 70"	0	0	0	0	0
"Max aceleration = 2, Speed = 80"	0	0	0	0	0
"Max aceleration = 2, Speed = 90"	0	0	0	0	0
"Max aceleration = 2, Speed = 100"	0	0	0	0	0
"Max aceleration = 2, Speed = 110"	0	0	0	0	0
"Max aceleration = 2, Speed = 120"	0	0	0	0	0
"Max aceleration = 2, Speed = 130"	0	0	0	0	0

4.2.1.2 Car to VRU scenario from standstill

Figure 4.6 shows severity levels for unintended acceleration in front of a VRU. Seen in the x-axis of the plot is the distance to the VRU from the car. As stated earlier the maximum distance for a pedestrian crossing is 5 meters which also is the upper limit. As seen in the figure there both severity levels of 1 and 2 can be seen. There is a change from s1 to s2 at 4m and allowed acceleration of $2m/s^2$, there is also a change at 1.5m and $6m/s^2$. FTTI value for S1 is 0.61s and 0.85s for s2.

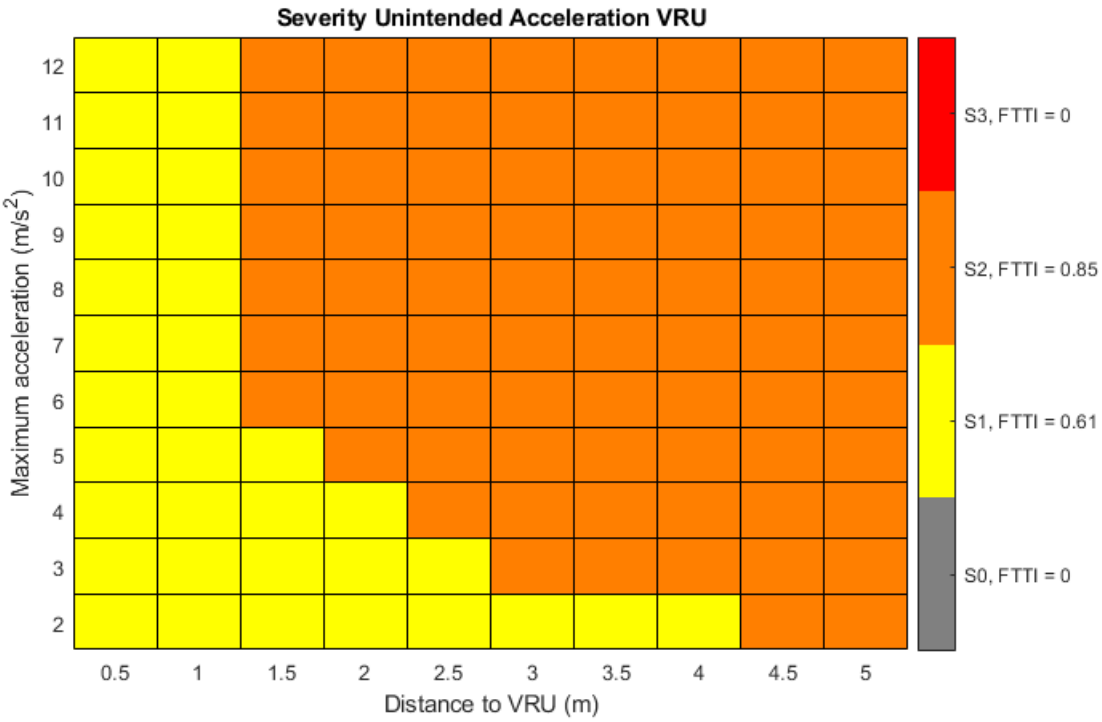

Figure 4.6: Severity estimation plot for unintended acceleration against VRU

4.2.2 Unintended deceleration

Following are the result from the scenarios with unintended deceleration, the two scenarios are as described earlier overbraking and underbraking. Overbraking is when the car brakes unintentionally and with a certain amount of deceleration. Underbraking is when the car braking with a lower-than-wanted declaration.

4.2.2.1 Overbraking

Figure 4.7 shows the same plot as for unintended acceleration but with initial speed and maximum allowed braking of the lead vehicle on the y-axis. The plot shows which severity is most likely to come from the scenario given an initial speed and allowed maximum deceleration. Together with the severity the shortest FTTI for each severity can also be seen. Values of FTTI can be seen as very similar for each category. This most likely should have relatively similar behaviour in the driver model and the increase in distance given from the initial speed and THW as speed is increased is compensated by the increased speed resulting in similar FTTI. For overbrakeing there can be seen a spread of severity values ranging from no-crash to S3. S3 cases can be seen at the higher speeds and allowed declaration and then S2 and S1 can be seen at the lower initial speeds and allowed deceleration. Mention above FTTI values are similar for all severity with S1 to S3 having 3.325 seconds as FTTI and S0 having 3.35 seconds.

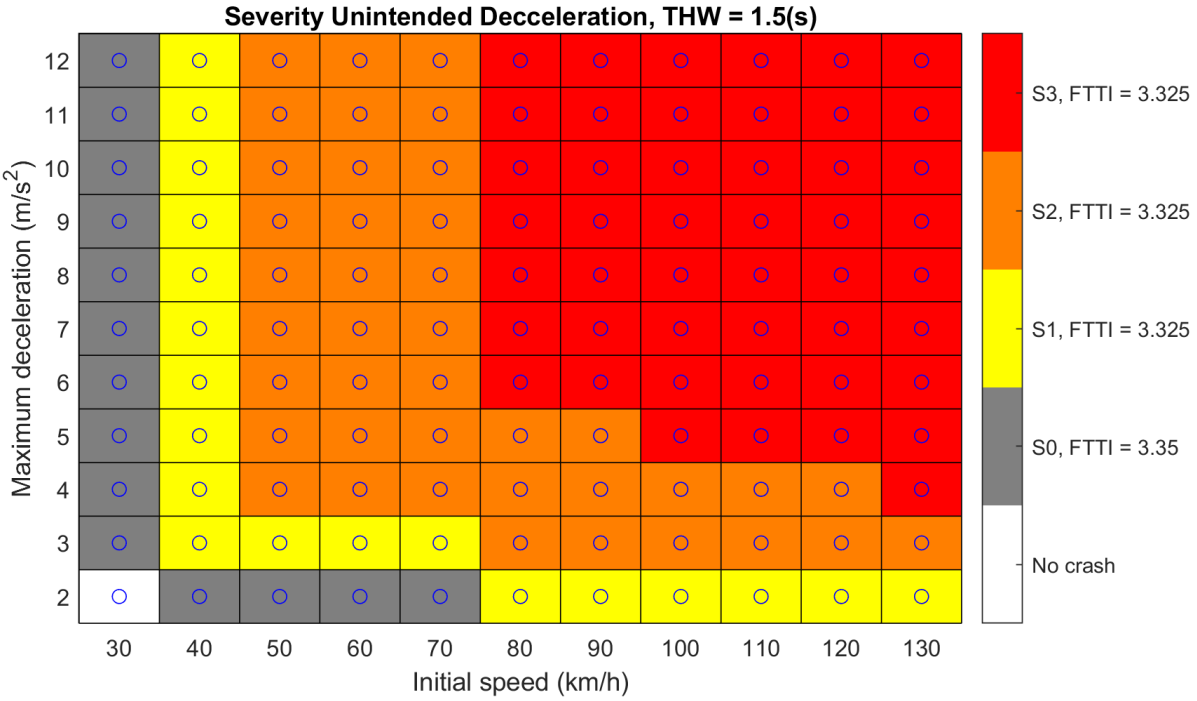

Figure 4.7: Plot showing severity and FTTI by initial speed and maximum allowed deceleration.

Table 4.2 shows the data used to get figure 4.7 Same as for the unintended acceleration, the severity is taken from the simulation resulting in the middle delta v crash speed. The FTTI values are taken from the same simulation as the severity.

Table 4.2: Severity and FTTI presented for the 10 first combinations of Brake cut-off deceleration and initial speed.

Case	S0	S1	S2	S3	FTTI
"Time Headway = 2, Speed = 30"	0.868	0.132	0	0	0
"Time Headway = 2, Speed = 40"	0.71	0.29	0	0	3.35
"Time Headway = 2, Speed = 50"	0.582	0.408	0.01	0	3.6
"Time Headway = 2, Speed = 60"	0.588	0.366	0.046	0	3.375
"Time Headway = 2, Speed = 70"	0.5	0.408	0.092	0	3.35
"Time Headway = 2, Speed = 80"	0.444	0.404	0.152	0	3.4
"Time Headway = 2, Speed = 90"	0.454	0.346	0.2	0	3.5
"Time Headway = 2, Speed = 100"	0.402	0.356	0.242	0	3.35
"Time Headway = 2, Speed = 110"	0.386	0.298	0.316	0	3.375
"Time Headway = 2, Speed = 120"	0.348	0.246	0.406	0	3.475
"Time Headway = 2, Speed = 130"	0.346	0.23	0.424	0	3.4

4.2.2.2 Underbraking

Figure 4.8 shows the severity plot for underbraking and corresponding FTTI values. Severity levels in this scenario are not as spread out as in the overbraking case where there were clear areas for different severities. From figure 4.8 S1 and S2 severities can be differentiated by speed at 40-50km/h while there are no clear borders between S2 and S3. There are some areas at high speed and high allowed braking which results in S2 and some S3 comes from lower speed and lower allowed braking, this at speed 130 and allowed deceleration of 9 and 12. FTTI values are also the same throughout all severities at 5.225 seconds.

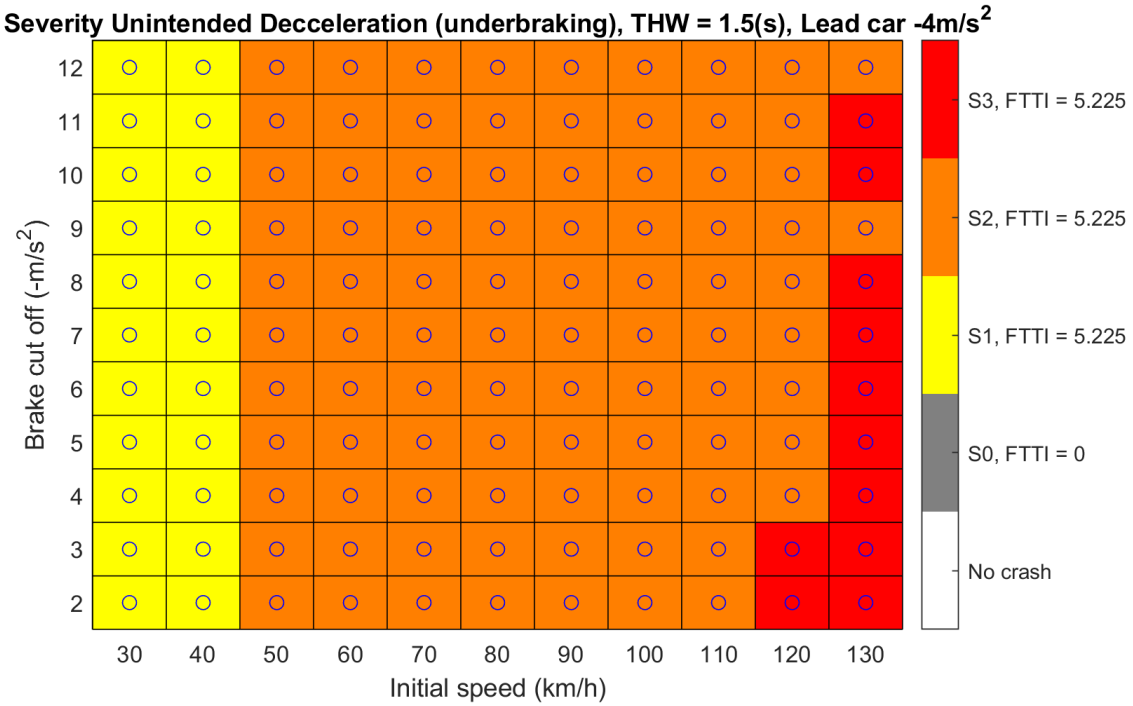

Figure 4.8: Plot showing severity and FTTI by initial speed and maximum given deceleration.

Table 4.3 shows the underlying data for the figure 4.8 The values shown in fig.. are taken in the same way as for previous result figures.

Table 4.3: Severity and FTTI presented for the 10 first combinations of Brake cut-off deceleration and initial speed.

Case	S0	S1	S2	S3	FTTI
"Brake Cut Off = 2, Speed = 30"	0.228	0.326	0	0	5.55
"Brake Cut Off = 2, Speed = 40"	0.088	0.468	0.222	0	5.475
"Brake Cut Off = 2, Speed = 50"	0.046	0.192	0.636	0	5.35
"Brake Cut Off = 2, Speed = 60"	0.034	0.172	0.74	0	5.975
"Brake Cut Off = 2, Speed = 70"	0.02	0.148	0.808	0	6.375
"Brake Cut Off = 2, Speed = 80"	0	0.098	0.896	0.006	5.35
"Brake Cut Off = 2, Speed = 90"	0	0.054	0.884	0.062	5.75
"Brake Cut Off = 2, Speed = 100"	0	0.006	0.826	0.168	5.3
"Brake Cut Off = 2, Speed = 110"	0	0	0.766	0.234	5.225
"Brake Cut Off = 2, Speed = 120"	0	0	0.46	0.54	5.7
"Brake Cut Off = 2, Speed = 130"	0	0	0.164	0.836	5.925

4.3 Severity comparison BEV and ICE

To investigate the potential differences and deviations between a conventional ICE vehicle compared to a BEV, multiple simulations in IPG CarMaker were set up. The simulations were set up to replicate a system fault resulting in an unintended acceleration of the vehicle to get an initial understanding of the potential difference in severity classification between the two propulsion setups.

For the comparison, two similar models were used one with BEV powertrain and one with ICE powertrain. The top performance model available for each propulsion setup was chosen to get a comparable result. Table 4.4 displays the vehicle performance data for the two configurations.

Table 4.4: Vehicle data for the ICE and BEV

Vehicle	**Mass [Kg]**	**Power[hp]**	**Torque[Nm]**
ICE	1771	247	350
BEV	2257	204 * 2	340 * 2

These two vehicles were simulated in CarMaker covering an unintended acceleration from a standstill. This type of scenario could represent a vehicle standing in front of a pedestrian crossing, waiting for a pedestrian to cross. For the severity assessment of a crash between a Car and a VRU the measure of impact speed is used to determine

the severity regardless of the vehicle mass. From the impact speed, a severity level can be determined according to internal standards at Volvo Cars.

Figure 4.9 shows the vehicle speed plotted against the distance travelled for the two propulsion setups. The plot shows that the potential impact speed between the car and the pedestrian doesn't differ that much in the typical range (two to five meters) for a car-pedestrian scenario described in section 2.2.4. Despite the larger torque availability for the BEV the behavior in the range from zero to five meters is very similar to the ICE. For larger distances above five meters, the behaviour starts to differ between the two setups, but these distances are not that relevant due to their uncommonness. This means that the severity assessment will not change between a BEV and ICE vehicle for the Car to pedestrian scenario with an unintended acceleration of the vehicle from a standstill.

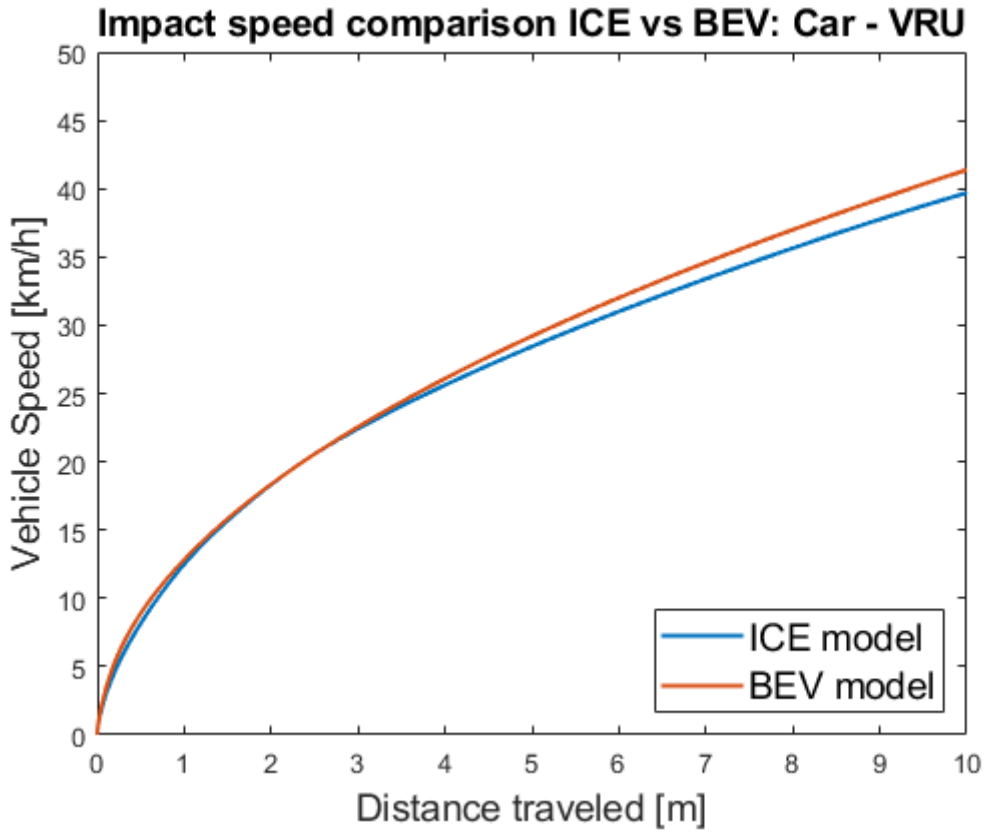

Figure 4.9: Impact speed plot comparison ICE and BEV.

Another interesting comparison between ICE and BEV is the unintended acceleration car to car scenario. This type of scenario could represent a queue situation where two vehicles are standing still facing the same direction with a certain distance between them. In the case of car to car scenario, the severity level is instead determined from delta velocity thresholds defined in internal standards at Volvo Cars. Delta velocity is defined in equation 4.1 as an inelastic collision between two bodies. ΔV_1 and ΔV_2 refer to the ΔV for the ego vehicle and the target vehicle respectively calculated based on mass(m) and vehicle velocity(V). For this thesis,

the target vehicle mass was set to 1000 kg representing a light passenger car and thereby representing the worst-case scenario with regard to delta velocity.

$$\Delta V_1 = \frac{m_2}{m_1 + m_2} \cdot (V_2 - V_1) \qquad \Delta V_2 = \frac{m_1}{m_1 + m_2} \cdot (V_1 - V_2) \tag{4.1}$$

Figure 4.10 shows the potential delta velocity plotted against the distance travelled for the two propulsion setups. The figure shows that the delta velocity starts to differ between the BEV and the ICE vehicle directly from the start. Due to the larger mass and increased acceleration capability of the BEV, the delta velocity increases more rapidly than the ICE setup. This results in a severity classification that could differ a lot between the BEV and ICE setup depending on the thresholds of the severity levels.

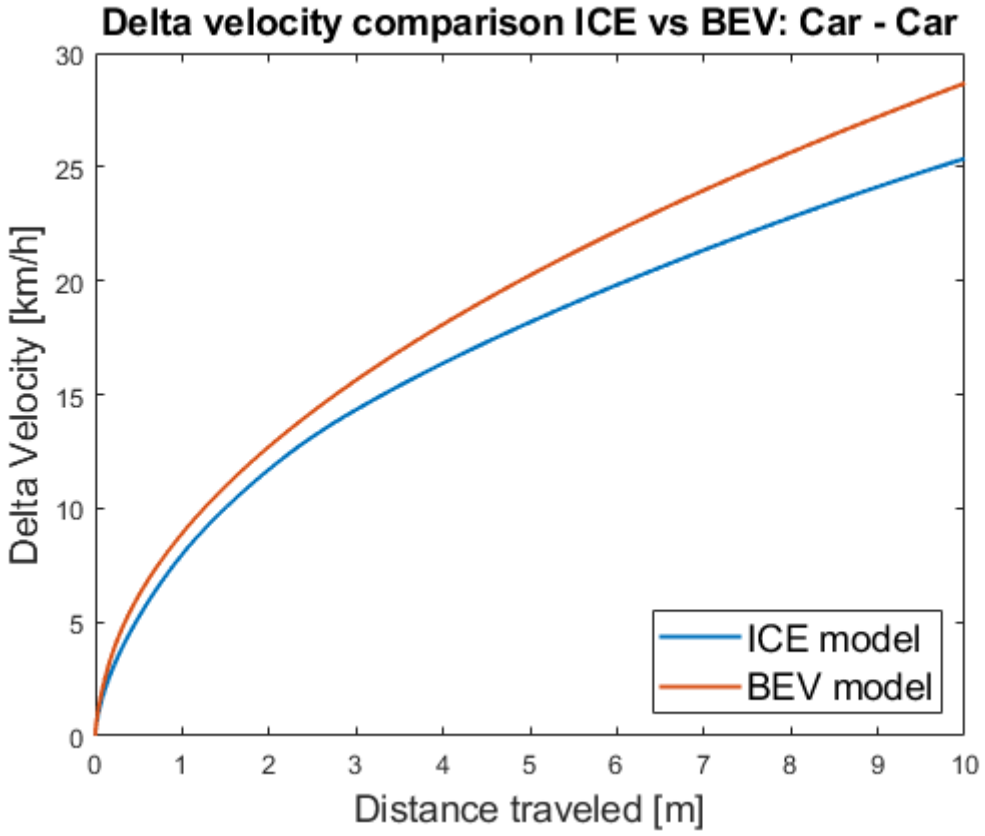

Figure 4.10: Delta velocity plot comparison ICE and BEV.

These results only contain an acceleration from zero and not acceleration capabilities from a rolling speed, but still give an indication that a BEV has the potential of causing higher severity classifications compared to an ICE vehicle. The main contributor to the higher severity classification was identified as the increased acceleration capabilities due to high torque availability and the often-higher mass of BEV vehicles.

Another aspect of the comparison justifying further that the BEV has the potential of creating more severe situations is the fact that the BEV most often lacks a gearbox. This results in a vehicle that can reach the full speed spectrum from 0 – 200 Km/h in the case of a system fault resulting in an unintended acceleration of the vehicle. In the case of a system fault in an ICE-powered vehicle the fault might cause an unintended acceleration but will most probably be limited by the gear it's currently running and thereby not reach as high speeds as the BEV. Depending on where the fault is occurring the ICE vehicle would most likely stay in the gear it's currently running.

4.3.1 Unintended acceleration comparison BEV and ICE

Following is a comparison between an ICE car and a similar BEV car to see the effect of the two different powertrains on safety. Seen in table 4.5 is the result from a BEV acceleration at a maximum of 12 m/s^2 from different speeds. Table 4.6 shows the same cases but for an ICE car. Seen in the tables are that FTTI is lower for the BEV in all cases. While the severity distrubtion can show that in general there are more S1 sevities for the BEV poertrain than for the ICE.

Table 4.5: Unintended acceleration in a BEV vehicle parented with Severity and FTTI for a maximum acceleration of 12 m/s^2

Max acceleration $[m/s^2]$	**Speed** $[km/h]$	**S0**	**S1**	**S2**	**S3**	**FTTI**
12	30	0.088	0.014	0	0	2.55
12	40	0.07	0.034	0	0	2.925
12	50	0.092	0.038	0	0	3.425
12	60	0.044	0.054	0	0	3.8
12	70	0.058	0.024	0	0	4.375
12	80	0.034	0.028	0.002	0	4.875
12	90	0.03	0.014	0.002	0	5.4
12	100	0.026	0.028	0	0	6.075
12	110	0.02	0.024	0.002	0	6.4
12	120	0.008	0.02	0	0	6.95
12	130	0.01	0.012	0	0	8

Table 4.6: Unintended acceleration in an ICE vehicle parented with Severity and FTTI for a maximum acceleration of 12 m/s^2

Max acceleration $[m/s^2]$	**Speed** $[km/h]$	**S0**	**S1**	**S2**	**S3**	**FTTI**
12	30	0.976	0.024	0	0	2.725
12	40	0.984	0.016	0	0	3.775
12	50	0.986	0.012	0.002	0	4.025
12	60	0.978	0.022	0	0	4.575
12	70	0.99	0.01	0	0	5.45
12	80	0.98	0.02	0	0	6.175
12	90	0.986	0.014	0	0	6.175
12	100	0.988	0.012	0	0	7.05
12	110	1	0	0	0	8.475
12	120	0.992	0.008	0	0	9.125
12	130	0.998	0.002	0	0	10.05

5

Discussion

The following chapter contains discussion about the results obtained from previous sections by first covering a discussion on changes in safety assessment when transitioning from ICE cars to BEVs, followed by an overall discussion of the result and various limitations of the model.

5.1 Safety discussion BEV and ICE

BEVs are in general heavier and more powerful than ICE cars which might cause more severe or critical situations on the road. As seen in the previous chapter there are some differences between ICE cars and BEV:s, even if the acceleration in general is similar between BEV:s and ICE. The weight difference of a BEV cause the ΔV to become higher on the other vehicle as it will absorb more of the energy. This can be seen in figure 4.10, where at around 1 meter a notable difference can be seen in ΔV.

The other comparison made between BEV and ICE is for unintended acceleration in a car following scenario. Tables 4.5 and 4.6 show the severity distribution and FTTI for BEV and similar ICE car. By comparing the tables it is evident that BEVs tend to have lower FTTI values. This is a crucial metric in system design, as it refers to the time elapsed from when a fault or error arises to the occurrence of a hazardous event, such as a crash in this context. Since the FTTI is lower for BEVs it means that fail-safe systems for BEVs need to detect failures and act on them faster than previously in ICE cars. Also in generally there more crashes with a severity of s1 for BEV then ICE which implies the crashes occurring with a BEV are more severe.

5.2 Simulation results

Overall the simulations show predicted results for the severity classification of scenarios and cases. Unintended acceleration shows no crashes which can be the result of using only the median delta v for classification. Since the driver model uses inverse tau as the measurement of urgency the closer the gap and higher delta velocity the more brake applied by the model. This probably results in that most simulation end in no crash as there will be a strong reaction from the drivermodel and acceleration

not being as strong as braking limiting the severity. For the VRU it's more straight forward with the severity increasing with distance to VRU.

Uninted declaration shows more severity as expected for both over and underbraking. This might be due to a car having similar braking performance at high and low speeds. For overbraking there can be seen a trend with higher severity for higher speeds This is as predicted as for higher speeds there is possible to achieve a higher crash speed and thus higher delta v at impact. The resolution for this simulation can also be considered to be good as trends appear where at different initial speeds and allowed deceleration severity changes. FTTI values remain similar this is interesting as it suggests that the initial speed and allowed deceleration does not affect the time it takes for a crash to occur.

Underbraking as mentioned briefly does also shows higher severity levels with s1-s3 being represented. As seen the severity seem to be purely dependent on initial speed instead of the combination of initial speed and allowed declaration. This can be a sign of low resolution, to get a better result the steps could be reduced specially the initial speeds. Another factor might be that the driver model dose not allow declaration values all the way up the set threshold meaning even if the car/model was allowed to brake more the driver model will limit it. When taking a single value from the model this can make quite the impact on the result. Some outliers can also been seen at $130km/h$, -9 and $-12m/s^2$ where there is a change in severity that seem suspicious, the most likely reason for this is as mention above that the results relay on a single value and therefore in some cases this might affect result as it lies as border point where there is a shift in severity around it. Meaning it can be close between that case being s2 or s3.

5.3 Limitations

Limitations exist for both the driver and vehicle model. Since the driver model is still relatively new and more comprehensive testing of it in cases like these would be beneficial to verify its performance and validity with simulations and comparisons to real-life data. The vehicle model is only consisting of basic kinematics which will yield some errors as seen so the result will differ from what could be expected behaviour of the real car. For example the model does not include any systems such as a real ABS system which most modern cars have now. Also in the model, there are no signal delays for example in the CAN system. This is a good thing since the model becomes more conservative and gives a worse result than in real life, but it needs to be highlighted as it affects the result. Simulation time limits the model as well since it would be preferable to run more simulations for each case and with a better resolution to understand where changes in severity levels happen. This was also briefly discussed in the previous section. Notable also is that in this report severity is assumed by taking the delta velocity between two vehicles meaning it considers the weight of the colliding vehicles but not their passive safety/crash worthiness. This makes the model more generic and simpler but can also affect the severity of the vehicles as for example a higher vehicle colliding with a lower one can

lead to that the collision becomes more severe due to how the strike each other.

5.4 Future work

Several steps and actions can be taken to further extend the scope of this project for further refinement and verification. The thesis has mainly focused on the scenarios for unintended deceleration and unintended acceleration in a car following scenario. The vehicle to pedestrian scenario has been included but not fully investigated. Current model design assumes that the pedestrian is standing still at the pedestrian crossing and does not react to the threat of an oncoming vehicle. By including a model of the pedestrian in the simulation model the pedestrian behavior could be used to define a controllability level. This model could for example be extended to be able to react to sound and in this way be used to evaluate the differences in reaction comparing a low-sounding vehicle compared to a nosier vehicle. The comparison between BEV vehicles and ICE vehicles could then further be investigated due to the sound difference between these two vehicle setups.

Further verification of the model needs to be done to secure the correct behaviour of the complete simulation model including, vehicle-, driver- and scenario- models. The vehicle model behaviour has been possible to verify both virtually in CarMaker and physically in the car, but the combination of driver and vehicle has not yet been verified. In order to verify this combination a study including a large set of test persons would be necessary. The test persons would then experience an injected fault in a car following scenario and then react to it. Preferably this type of test would be executed on a test track but due to the high safety risk of performing a study like this a vehicle simulator might have been more suitable.

For the BEV vs ICE comparison, state of charge (SOC) dependent acceleration capabilities can be investigated for further analysis. The SOC for a BEV could potentially have an impact on the acceleration capabilities of the vehicle. This could result in a lower or worse severity in the case of a fault depending on the SOC level. If SOC has an impact on the acceleration capabilities a distribution and probability of SOC level could be used as a part of defining an exposure level.

Using the driver model has resulted in a simulation that is computationally costly since each scenario combination needs to be simulated at least 1000 times to get a driver response distribution. Further work needs to be focused on improving the computation time in order to get a more accessible tool that can provide fast results.

6

Conclusion

This thesis has developed a vehicle model to simulate the behaviour of a car using data that is accessible early in the development process. Implemented a new generation of driver models developed using naturalistic data that capture driver's responses more realistically in safety-critical situations. Combining the vehicle model with the driver model, this thesis has evaluated different longitudinal hazardous situations involving unintended acceleration both car to car and car to VRU, as well as car to car deceleration situations. Evaluation of each scenario has been done via ASIL classifications and through key metrics within functional safety such as FTTI.

The main conclusion from this thesis is that an introduction of electric propulsion systems will change the severity classification in common longitudinal scenarios regarding acceleration both car to car and car to VRU compared to previous ICE drivetrains. Due to the increased acceleration capability and increased mass, the severity classification will in some cases rise to a higher level, but the biggest difference can be seen in the measure of FTTI. FTTI for an unintended acceleration car to car case could be up to 2 seconds longer for an ICE vehicle compared to a BEV.

During the development of the vehicle model, some conclusions could be made regarding the complexity level required to get an accurate result. During acceleration the most important factor where the build-up time to reach maximum torque at the wheels, this is limited by factors such as how fast the batteries are allowed to ramp up current and the dynamics of the powertrain with drive axles. While for declaration the dynamics of the car are of more importance, behaviours such as load transfers between front and rear wheels as well as suspension dynamics. But since these dynamics are more complex and need input data from suspension design, it might not be available at the time during the development of a new car when this model is supposed to be used the model excluded suspension modelling.

Bibliography

Aptiv. (n.d.). *What is asil-d?* (Aptiv., Ed.). Retrieved January 23, 2023, from https://www.aptiv.com/en/insights/article/what-is-asil-d

Bärgman, J., Boda, C.-N., & Dozza, M. (2017). Counterfactual simulations applied to shrp2 crashes: The effect of driver behavior models on safety benefit estimations of intelligent safety systems. *Accident Analysis & Prevention*, *102*, 165–180. https://doi.org/https://doi.org/10.1016/j.aap.2017.03.003

Becker, C., Nasser, A., & Attioui, F. (2020). *Functional safety assessment of a generic accelerator control system with electronic throttle control in electric vehicles* (Tech Report DOT HS 812 656;DOT-VNTSC-NHTSA-15-13). United States. Department of Transportation. National Highway Traffic Safety Administration. Washington, DC: United States. https://rosap.ntl.bts.gov/view/dot/44158

Bengt J H Jacobson. (2020). *Vehicle dynamics compendium* (tech. rep.). Chalmers, Mechanics, Maritime Sciences (M2), Vehicle Engineering, and Autonomous Systems. Gothenburg, SE. https://research.chalmers.se/en/publication/513850

Fabris, S., & Lovric, T. (2012). Method for hazard severity assessment for method for hazard severity assessment for the case of undemanded deceleration - simone fabris. https://doi.org/10.13140/RG.2.2.15043.22568

Fambro, D. B., Fitzpatrick, K., & Koppa, R. J. (1997). *Determination of stopping sight distances* (Vol. 400). Transportation Research Board.

Green, M. (2000). "how long does it take to stop?" methodological analysis of driver perception-brake times. *Transportation Human Factors*, *2*, 195–216. https://doi.org/10.1207/STHF0203_1

Høye, A. K. (2017). *Road safety effects of vehicles crashworthiness, weight, and compatibility* (No. 1580/2017). toi.no/publications/road-safety-effects-of-vehicles-crashworthiness-weight-and-compatibility-article34633-29.html

Hughes, A., & Drury, B. (2019). Chapter 9 - synchronous, permanent magnet and reluctance motors and drives. In A. Hughes & B. Drury (Eds.), *Electric motors and drives (fifth edition)* (Fifth Edition, pp. 307–373). Newnes. https://doi.org/https://doi.org/10.1016/B978-0-08-102615-1.00009-X

International Electrotechnical Commission. (2010). *Iec 61508:2010 functional safety of electrical/electronic/programmable electronic safety-related systems* (Standard IEC 61508:2010). International Electrotechnical Commission. Geneva, CH. https://webstore.iec.ch/publication/22273

IPG Automotive GmbH. (2021). *Ipg carmaker* (Version 9.1.2). https://ipg-automotive.com/en/products-solutions/software/carmaker/

ISO Central Secretary. (2018). *Iso 26262-1:2018 road vehicles — functional safety* (Standard ISO 26262-1:2018). International Organization for Standardization. Geneva, CH. https://www.iso.org/standard/68383.html

Johansen, A. (2010). Monte carlo methods. In P. Peterson, E. Baker, & B. McGaw (Eds.), *International encyclopedia of education (third edition)* (Third Edition, pp. 296–303). Elsevier. https://doi.org/https://doi.org/10.1016/B978-0-08-044894-7.01543-8

Liu, C., Zhao, L., & Lu, C. (2022). Exploration of the characteristics and trends of electric vehicle crashes: A case study in norway. *European Transport Research Review*, *14*(1), 6. https://doi.org/10.1186/s12544-022-00529-2

Pacejka, H. B. (Ed.). (2012). In *Tire and vehicle dynamics (third edition)* (Third Edition, p. iv). Butterworth-Heinemann. https://doi.org/https://doi.org/10.1016/B978-0-08-097016-5.02001-5

SÜD, T. (n.d.). *Functional safety overview* (TÜV SÜD, Ed.). Retrieved January 23, 2023, from https://www.tuvsud.com/en-us/services/functional-safety/about

Svärd, M., Markkula, G., Engström, J., Granum, F., & Bärgman, J. (2017). A quantitative driver model of pre-crash brake onset and control. *Proceedings of the Human Factors and Ergonomics Society Annual Meeting*, *61*(1), 339–343. https://doi.org/10.1177/1541931213601565

Taieb-Maimon, M., & Shinar, D. (2001). Minimum and comfortable driving headways: Reality versus perception [PMID: 11474761]. *Human Factors*, *43*(1), 159–172. https://doi.org/10.1518/001872001775992543

The MathWorks Inc. (2021). *Matlab* (Version r2021b). https://se.mathworks.com/products/matlab.html

Trafikverket. (2020). *Råd - vgu, vägars och gators utformning* (Standard 2020:031). Trafikverket. Borlänge, SE.

WINSUM, W. V., & HEINO, A. (1996). Choice of time-headway in car-following and the role of time-to-collision information in braking [PMID: 8854979]. *Ergonomics*, *39*(4), 579–592. https://doi.org/10.1080/00140139608964482

A

Appendix

Following are the full set of equations used in the magic formula. This thesis uses the pure longitudinal formula since it is only interested in acceleration and deceleration in a straight line. Scaling factors λ are all set to equal 1 as well as turn slip parameter ζ_1.

$$F_{x0} = D_x sin[C_x atan B_x \kappa_x - E_x(B_x\kappa_x) - atan(B_x\kappa_x)] + S_{Vx} \tag{A.1}$$

$$\kappa_x = \kappa + S_{Hx} \tag{A.2}$$

$$C_x = \rho_{Cx1} \cdot \lambda_{Cx} \tag{A.3}$$

$$D_x = \mu_x \cdot F_z \cdot \zeta_1 \tag{A.4}$$

$$\mu_x = (\rho_{Dx1} + \rho_{Dx2} df_z) \cdot (1 - \rho_{Dx3}\gamma_x^2) \cdot \lambda_{\mu x} \quad (> 0) \text{ with } \gamma_x = \gamma \cdot \lambda_{\gamma x} \tag{A.5}$$

$$E_x = (\rho_{Ex1} + \rho_{Ex2} df_z + \rho_{Ex2} df_z^2) \cdot (1 - \rho_{Ex4} sgn(\kappa_x)) \cdot \lambda_{Ex} \tag{A.6}$$

$$K_{x\kappa} = F_z \cdot (\rho_{Kx1} + \rho_{Kx2} df_z) \cdot exp(\rho_{Kx3} df_z) \cdot \lambda_{Kx\kappa} \tag{A.7}$$

$$B_x = \frac{K_{xk}}{C_x D_x + \epsilon_x} \tag{A.8}$$

$$S_{Hx} = (\rho_{Hx1} + \rho_{Hx2} df_z) \cdot \lambda_{Hx} \tag{A.9}$$

$$S_{vx} = F_z \cdot (\rho_{Vx1} + \rho_{Vx2} df_z) \cdot \lambda_{Vx} \cdot \lambda_{\mu x} \cdot \zeta_1 \tag{A.10}$$

$$df_z = \frac{F_x - F'_{z0}}{F'_{z0}} \tag{A.11}$$

$$F'_{z0} = \lambda_{F_{z0}} F_{zo} \tag{A.12}$$

DEPARTMENT OF MECHANICS AND MARITIME SCIENCES
CHALMERS UNIVERSITY OF TECHNOLOGY
Gothenburg, Sweden
www.chalmers.se

CHALMERS
UNIVERSITY OF TECHNOLOGY